

## General Disclaimer

### One or more of the Following Statements may affect this Document

- This document has been reproduced from the best copy furnished by the organizational source. It is being released in the interest of making available as much information as possible.
- This document may contain data, which exceeds the sheet parameters. It was furnished in this condition by the organizational source and is the best copy available.
- This document may contain tone-on-tone or color graphs, charts and/or pictures, which have been reproduced in black and white.
- This document is paginated as submitted by the original source.
- Portions of this document are not fully legible due to the historical nature of some of the material. However, it is the best reproduction available from the original submission.

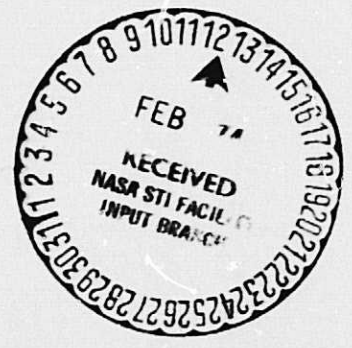
N74-14190 Pt. 1 ~~86072~~ -74  
N73-33430 Pt. 2 ~~14876~~ -73

NASA-CR-121261) HIGH TEMPERATURE, LOW  
CYCLE FATIGUE OF COPPER-BASE ALLOYS IN  
ARGON. PART 3: ZIRCONIUM-COPPER;  
(Mar-Test, Inc., Cincinnati, Ohio.)  
HC \$4.75

N74-16209

52 p  
CSCL 1iP G3/17  
Unclas  
27979

NASA CR-121261



HIGH TEMPERATURE, LOW CYCLE FATIGUE  
OF COPPER-BASE ALLOYS IN ARGON;  
PART III - ZIRCONIUM-COPPER; THERMAL-  
MECHANICAL STRAIN CYCLING, HOLD-TIME  
AND NOTCH FATIGUE RESULTS

by: J.B.Conway, R.H.Stentz and J.T.Berling

MAR-TEST INC.

Cincinnati, Ohio

December, 1973

prepared for

NATIONAL AERONAUTICS AND SPACE ADMINISTRATION

NASA Lewis Research Center  
Contract NAS3-16753

G.R.Halford, Project Manager

1. Report No.	2. Government Accession No.	3. Recipient's Catalog No.	
4. Title and Subtitle High Temperature, Low-Cycle Fatigue of Copper-Base Alloys in Argon; Part III- Zirconium-Copper; Thermal-Mechanical Strain Cycling, Hold-Time and Notched Bar Fatigue Results.		5. Report Date December, 1973	6. Performing Organization Code
7. Author(s) J.B. Conway, R.H. Stentz and J.T. Berling		8. Performing Organization Report No. MTI-RG03-2-3	10. Work Unit No.
9. Performing Organization Name and Address Mar-Test Inc. 45 Novner Drive Cincinnati, Ohio 45215		11. Contract or Grant No. NAS3-16753	13. Type of Report and Period Covered Contractor Report October through Dec., 1973
12. Sponsoring Agency Name and Address National Aeronautics and Space Administration Lewis Research Center 21000 Brookpark Rd., Cleveland, Ohio 44135		14. Sponsoring Agency Code	
15. Supplementary Notes Project Manager, Dr. G. Halford, NASA-Lewis Research Center Cleveland, Ohio			
16. Abstract The low-cycle fatigue characteristics of smooth bar and notched bar specimens (hourglass shape) of zirconium-copper, 1/2 Hard, material (R-2 Series) were evaluated at room temperature in axial strain control. Over the fatigue life range from about 300 to 3000 cycles the ratio of fatigue life for smooth bar to fatigue life for notched bar remained constant at a value of about 6.0. Some additional hold-time data for the R-2 alloy tested in argon at 538°C are reported. Hold period durations to 300 seconds were employed in tests involving a hold period in tension only, compression only, and in both tension and compression. These tests were performed to study the effects of hold period durations which were longer than those employed in the previous task. An analysis of the relaxation data obtained in these hold-time tests is also reported and it is shown that these data yield a fairly consistent correlation in terms of instantaneous stress rate divided by instantaneous stress. Two thermal-mechanical strain cycling tests were also performed using a cyclic frequency of 4.5 cycles per hour and a temperature cycling interval from 260° to 538°C. The fatigue life values in these tests were noticeably lower than that observed in isothermal tests at 538°C. It also appeared that the most detrimental condition was that in which the peak temperature occurred at the peak tensile strain point in the cycle. Tensile and fatigue data are reported for a second lot of the zirconium-copper (1/2 Hard) alloy.			
17. Key Words (Suggested by Author(s)) Fatigue, Tensile, Hold-time, Relaxation, Smooth Bar, Notched Bar, Thermal-Mechanical, Zirconium-Copper.		18. Distribution Statement unclassified-unlimited	
19. Security Classif. (of this report) unclassified	20. Security Classif. (of this page) unclassified	21. No. of Pages	22. Price*

\* For sale by the National Technical Information Service, Springfield, Virginia 22151

## TABLE OF CONTENTS

	<u>page</u>
I- SUMMARY	1
II- INTRODUCTION	3
III- MATERIAL AND SPECIMENS	7
IV- TEST EQUIPMENT	12
V- TEST PROCEDURES	17
A) Low-cycle Fatigue	17
B) Short-term Tensile	20
C) Thermal-mechanical	21
VI- TEST RESULTS AND DISCUSSION OF RESULTS	24
A) Short-term Tensile	24
B) Low-cycle Fatigue	24
1) Smooth bar versus notched bar	24
2) Second lot of zirconium-copper alloy	24
3) Hold-time effects	32
C) Thermal-mechanical Strain Cycling	42
VII- CONCLUSIONS	46
 DISTRIBUTION LIST FOR THIS REPORT	 50

## I- SUMMARY

This report describes the test results obtained in the Task 3 portion of this program and represents the final report on this program. In this phase of the testing effort a comparison of smooth bar and notched bar fatigue life was obtained for zirconium-copper, 1/2 Hard, material tested in air at room temperature in axial strain control. These data indicated that the ratio of smooth bar fatigue life to notched bar fatigue life was constant at about 6.0 over the life regime between 300 and 3000 cycles. Data at five different strain ranges were employed in these evaluations.

Five additional hold-time tests were performed in argon at 538°C using a ramp strain rate of  $2 \times 10^{-3} \text{ sec}^{-1}$ . These tests supplement the hold-time data previously reported for the R-2 alloy and focused on hold-period durations of 300 seconds. Evaluations were made using a hold period in tension only, a hold period in compression only, and a hold period in both the tension and compression portions of the cycle. A significant amount of dimensional instability was encountered in these tests and this made it difficult to obtain a completely reliable assessment of the hold-time effect.

Relaxation data obtained in the first few cycles of the hold-time tests were analyzed in terms of an instantaneous stress rate correlation and fairly consistent results were obtained. This analysis also indicated that, at the same stress level, the relaxation rate in tension was definitely faster than that observed in compression.

Short-term tensile data at room temperature and 538°C and low-cycle fatigue data at 538°C were obtained for a second lot of zirconium-copper (1/2 Hard) material. These data indicated noticeably lower yield and ultimate strengths at both room temperature and 538°C for this second lot of material (designated R-20) compared to the results reported in the Task 2 portion of this program for the R-2 material. However, the low-cycle fatigue properties for the R-20 material at 538°C were essentially identical to those reported for the R-2 material although there was some indication that the R-20 material was yielding somewhat greater fatigue life values at the lower strain ranges.

Two thermal-mechanical strain cycling tests were performed in an evaluation of the R-2 material. These tests employed a cyclic frequency of 4.5 cycles per hour and a cyclic temperature interval from 260° to 538°C. One test involved

having the maximum temperature occur at the peak tensile strain point in the cycle and the minimum temperature at the peak compressive strain point. In the second test this phase relationship was reversed. Both tests yielded a fatigue life lower than that observed in isothermal fatigue tests at  $538^{\circ}\text{C}$  for this material. It was also noted that the condition involving the maximum temperature at peak tensile strain was more detrimental than the reversed phase relation.

## II - INTRODUCTION

Regeneratively-cooled, reusable-rocket nozzle liners such as found in the engines of the Space Shuttle, Orbit-to-Orbit Shuttle, Space Tug, etc., undergo a severe thermal strain cycle during each firing. To withstand the severe cycles, the liner material must have a proper combination of high thermal conductivity and high low-cycle fatigue resistance. Copper-base alloys possess these desirable qualities and were thusly chosen for this program. The purpose of the investigation is to screen a variety of candidate alloys, select the most promising for the application, and to generate material property data that are required in the design and life prediction of rocket nozzle liners.

In the Task 1 effort (see NASA CR 121259) on this program a detailed screening evaluation was performed to provide an assessment of the tensile and fatigue properties of 12 candidate materials (11 copper-base alloys and silver) at temperatures to 538°C. Short-term tensile tests were performed in duplicate using a strain rate of  $2 \times 10^{-3} \text{ sec}^{-1}$  to provide measurements of the 0.2% yield strength, ultimate tensile strength and reduction in area at room temperature and at 538°C. Low-cycle fatigue evaluations were performed at 538°C using an axial strain rate of  $2 \times 10^{-3} \text{ sec}^{-1}$  in completely reversed (R-ratio of infinity), axial strain controlled tests based on axial loading. All room temperature evaluations were performed in air while all tests at 538°C were performed in high purity argon in which the oxygen level was maintained below 0.01 percent by volume. Hourglass-shaped specimens and diametral extensometry were employed in both the tensile and fatigue evaluations while the use of an analog strain computer enabled the fatigue tests to be performed in axial strain control.

After the Task 1 effort was completed the NASA Project Manager performed a detailed review of all the material property information pertaining to the 12 candidate materials and selected one material to be tested in additional detail in the Task 2 portion of this program. This material was the R-2 alloy, zirconium-copper, 1/2 Hard.

The material property measurements specified for the Task 2 effort included the following:

- 1) short-term tensile at 482° and 593°C using a strain rate of  $2 \times 10^{-3} \text{ sec}^{-1}$ ;
- 2) short-term tensile at 538°C using strain rates of

- $4 \times 10^{-4}$  and  $1 \times 10^{-2}$  sec<sup>-1</sup>;  
 3) modulus of elasticity from room temperature to 593°C using a strain rate of  $2 \times 10^{-3}$  sec<sup>-1</sup>;  
 4) strain-controlled low-cycle fatigue behavior at 482° and 593°C  
 5) strain-controlled low-cycle fatigue behavior at 538°C using strain rates of  $4 \times 10^{-4}$  and  $1 \times 10^{-2}$  sec<sup>-1</sup>;  
 and 6) strain-controlled low-cycle fatigue behavior at 538°C to evaluate the effect of hold periods in tension and in compression

All the tensile and fatigue tests were performed in argon using hourglass-shaped specimens while all the modulus of elasticity measurements were performed in air using cylindrical gage section specimens. A servo-controlled, hydraulically actuated fatigue testing machine was used in all these evaluations and the threaded test specimens were mounted in the holding fixtures of the test machine using special threaded adaptors. For the environmental (argon) tests a specially constructed pyrex containment vessel was positioned between the holding fixtures of the fatigue machine and neoprene low-force bellows at either end provided the seal to enable the desired gas purity levels to be maintained throughout the test. Side outlets (with appropriate seals) on this containment vessel provided entrance ports to accommodate the extensometer arms and special lead-throughs near the bottom of the containment vessel enabled the thermocouples, used for specimen temperature measurement, to be routed out to the temperature control system. Specimen test temperatures were attained using induction heating and this was provided by winding a closely spaced induction coil around the outer surface of the cylindrical containment vessel (see Figure 1).

All force measurements were made using a load cell mounted within the loading train of the fatigue machine and specimen strains were measured using specially designed, high temperature extensometers. For the short-term tensile and fatigue evaluation a diametral extensometer was employed while an axial extensometer was used in the modulus of elasticity determinations. A special test procedure was developed to allow the short-term tensile tests to be performed at a constant strain rate which was maintained throughout the test. In the fatigue tests an analog strain computer was employed which allowed the diametral strain signal to be used in conjunction with the load signal so as to provide an instantaneous value for the axial strain which was then the controlled variable. When the modulus measurements were made the axial extensometer was attached to the cylindrical test specimen (gage length of 1.27 cm) and then the specimen was loaded within the elastic region while a plot was made of the corresponding load and axial strain information. A slope calculation of this record yielded the desired modulus value.

The studies performed in the Task 2 effort to define



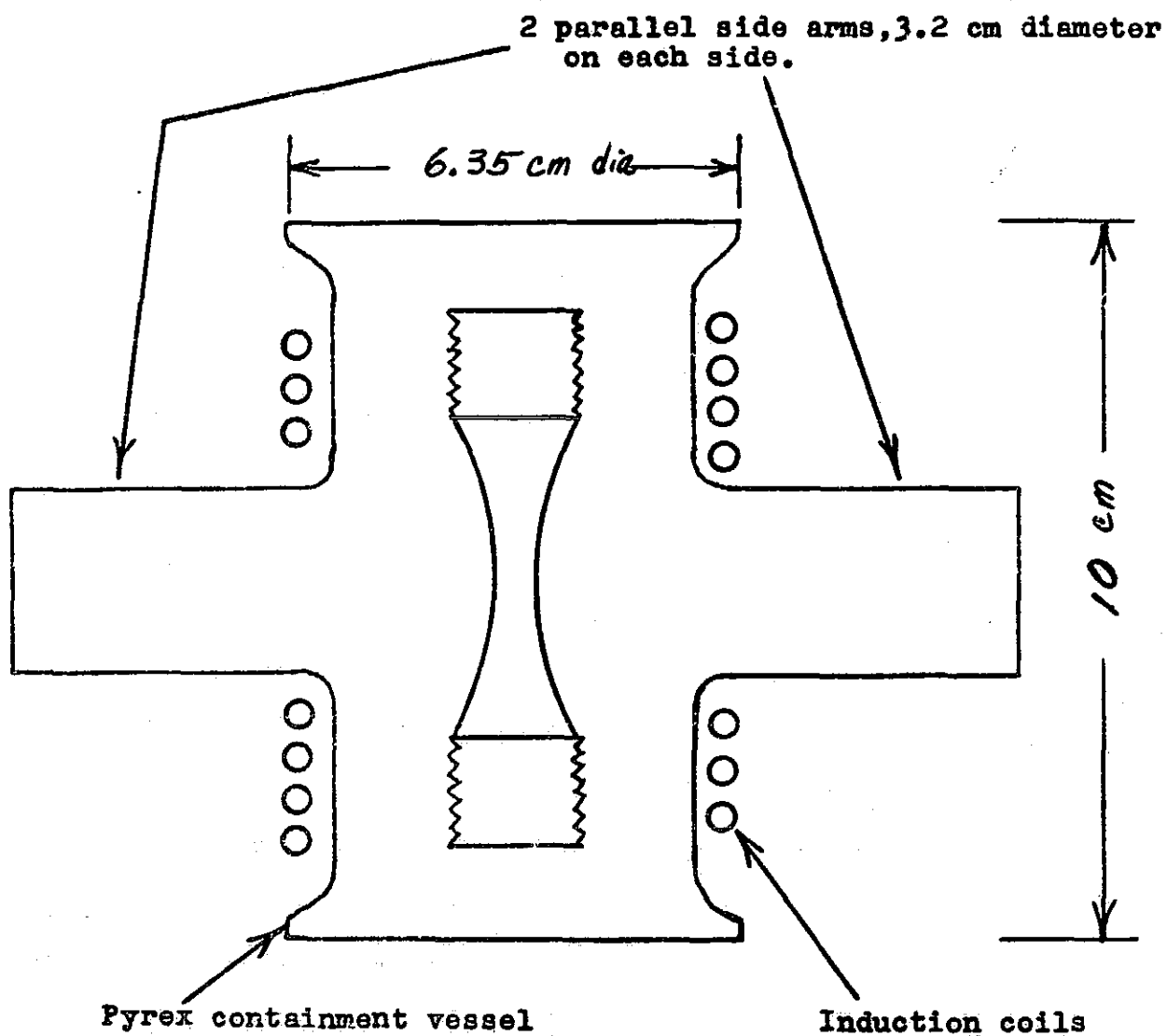


Figure 1- Schematic of Pyrex Environmental Test Chamber.

temperature, strain-rate and hold-time effects yielded some important information for the R-2 alloy. Some general observations of special interest included:

- 1) the 0.2% yield strength and ultimate tensile strength of the R-2 alloy decrease gradually with increasing temperature and vary from about 340 and 380 MN/m<sup>2</sup> respectively at room temperature to about 150 and 160 MN/m<sup>2</sup> at 593°C; the reduction in area increases gradually to about 90% as the temperature is increased to 593°C;
- 2) the tensile properties of the material were not significantly affected by strain rate at 538°C over the range from  $4 \times 10^{-4}$  to  $1 \times 10^{-2}$  sec<sup>-1</sup>;
- 3) the modulus of elasticity decreased from about 115,000 to 70,000 MN/m<sup>2</sup> over the temperature range from room temperature to 593°C;
- 4) The R-2 alloy exhibited a very decided cyclic strain softening;
- 5) the fatigue life at a strain rate of  $2 \times 10^{-3}$  sec<sup>-1</sup> was unaffected by temperature over the range from 482° to 593°C;
- 6) the fatigue life at 538°C was decreased as the strain rate decreased;
- 7) the fatigue life at 538°C was decreased by hold periods in tension; hold periods in compression exerted essentially no effect on the fatigue life;
- 8) the amount of stress relaxation which occurred during a tension hold period was the same as that observed in a compression hold period of the same duration;
- 9) after the first fatigue cycle or so the ratio of the stress decrease due to relaxation to the stress level at the start of the hold period remained essentially constant throughout the test.

The final portion (Task 3) of this program was devoted to further evaluations of the R-2 composition. Attention was focused first on a comparison of the low-cycle fatigue characteristics of smooth and notched ( $K_t = 2$ ) bars at room temperature using axial strain control, and on extending the hold-time studies initiated in the Task 2 portion of this program. Two thermal-mechanical strain cycling evaluations were also performed to provide a limited assessment of this facet of fatigue behavior. And, finally, some indication of lot-to-lot variation was obtained in tests of a second lot of the zirconium-copper, 1/2 hard, composition. This alloy was designated, R-20, and was subjected to the same tensile and low-cycle fatigue tests specified in the test matrix of Task 1.

### III - MATERIAL AND SPECIMENS

Specimen material for use in this portion of the program was supplied by NASA-Lewis Research Center, Cleveland, Ohio. The two lots (designated R-2 and R-20) of zirconium-copper alloy employed in this study are described in Table 1.

Using the specimen design shown in Figure 2, 16 specimens were fabricated from the R-2 material and 17 from the R-20 material. In addition, 6 specimens of the design shown in Figure 3 were fabricated from the R-2 material for use in the evaluation of notched-bar behavior. No evaluation of the notched behavior of the R-20 material was required in this program.

A photograph of the smooth and notched specimens employed in this program is presented in Figure 4.

After being machined, all specimens were wrapped in soft tissue paper and placed in individual hard plastic cylinders (about 9 cm in length and 2.2 cm inside diameter). The ends of these cylinders were then sealed with masking tape and the specimen code number was written on the external surface of the cylinder. These cylinders were used for storage before and after test.

In preparing for a test each specimen was subjected to the following:

- 1) a small longitudinal notch was filed in the threaded sections of the specimen; this was designed to aid in the removal of entrapped air from the threaded area after the specimen was inserted in the adaptors (see below for specimen-adaptor assembly);
- 2) the specimen was washed with Freon to remove any surface oils which might have remained after machining;
- 3) a small quantity of dilute phosphoric acid was applied by hand to the complete surface of the specimen; this removed any surface oxides and any machining oil not removed by the cleaning with Freon; this operation was completed within 15 seconds;
- 4) the specimen was rinsed in warm water and dried using soft absorbent tissue;
- 5) the specimen was then subjected to a final cleaning with Freon.

Table 1 - Source History for R-2 and R-20 Zirconium-Copper Alloy

	R-2	R-20
Source	Bridgeport Brass Co. Mill Order No. 98700	United States Metal Refining Co.  Lot No. H-6932
Form	1.90 cm diameter round bars (had received a 50% reduction in area plus aged)	390 pound billets which were reduced to 2.86 cm diameter rods; following annealing these rods were cold reduced to 2.3 cm diameter rods which were then further cold reduced by NASA-Lewis Research Center to 2.03 cm to give a 50% reduction in area from the 2.86 cm diameter
Condition	1/2 Hard	1/2 Hard
Composition (wt %)	Zr 0.20 Ni 0.002 Fe 0.002 Cu Balance	Zr 0.13 to 0.19 nominal Balance Cu

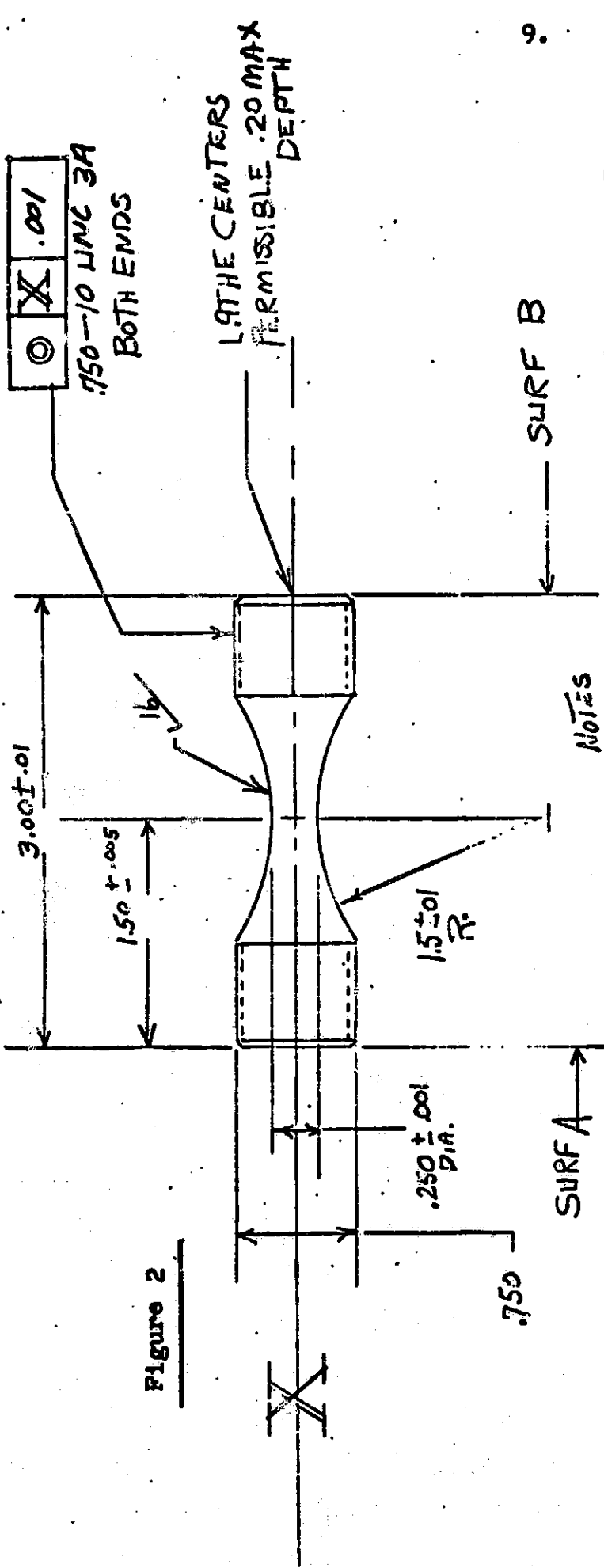


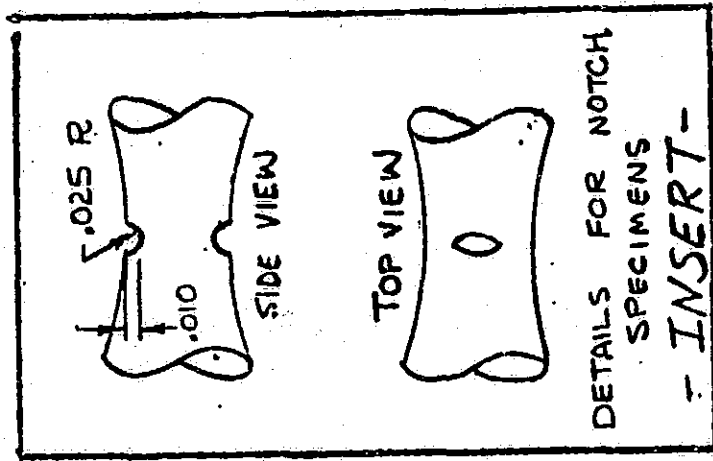
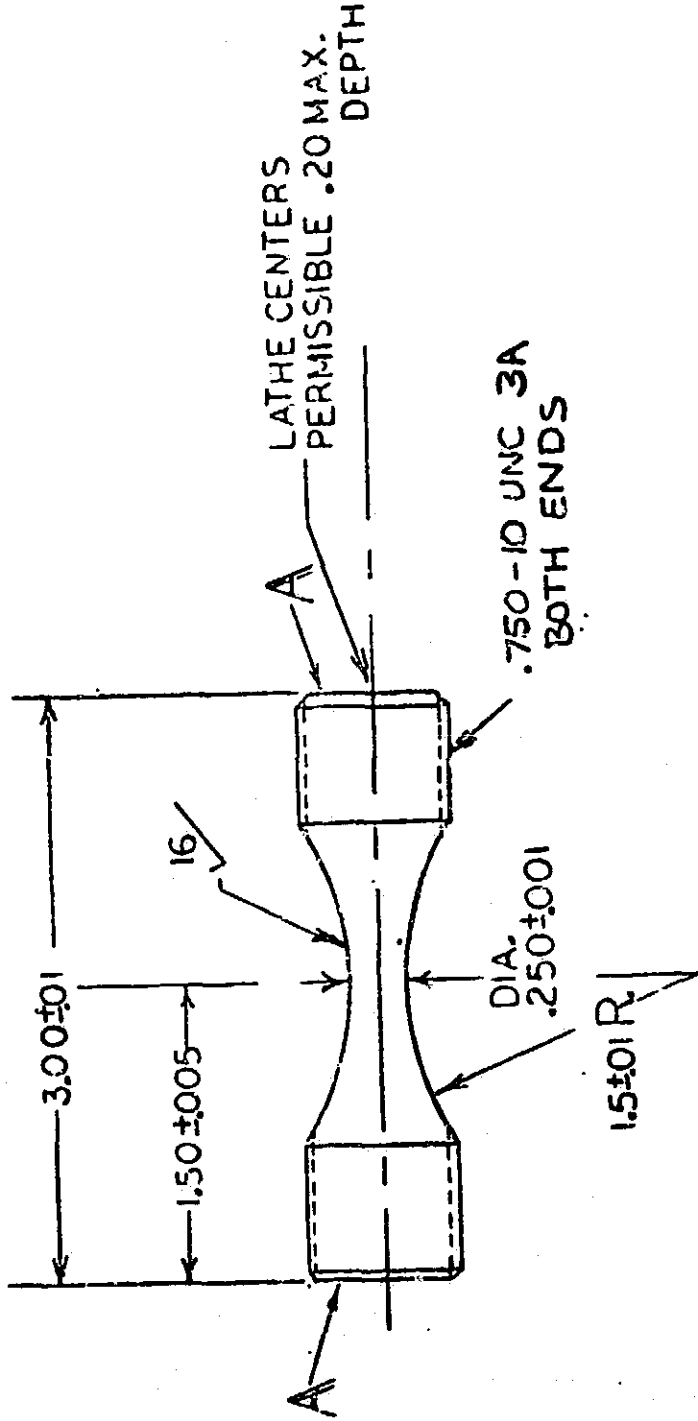
Figure 2

5- SCREW THREADS TO BE AS LISTED IN NBS HAND BOOK H 28

NOTES

- 1- SURFACES A, & B TO BE PARALLEL WITHIN .001
- 2- SURFACES A, & B TO BE PERPENDICULAR TO CENTER LINE OF SPECIMEN WITHIN .0005 TIR
- 3- CONTOURED PORTION OF SPECIMEN TO HAVE A  $\sqrt{R}$  FINISH OR BETTER. FINISHING SHOULD BE IN THE AXIAL DIRECTION USING LOW STRESS LAPPING OR POLISHING OPERATION
- 4- ALL DIMS TO BE CONCENTRIC WITHIN .001

UNLESS OTHERWISE SPECIFIED DIMENSIONS ARE IN INCHES TOLERANCES ON FRACTIONS DECIMALS ANGLES ± ± ±	DRAWN	SPECIMEN		Mar-Test inc. CINCINNATI, OHIO
	DATE	Low CYCLE FATIGUE		
APPD	ISSUED	SCALE 1/1	WT CALC	CONT ON SHEET
ENGR <i>STC</i>	APPROVED <i>STC</i>		ACTUAL	
MFG	DATE 1-12-71			SH NO.
MATL				MTI-1002
ALL SURFACES ±				
MATERIAL				
30VT. OR COM. TO BE SPECIFIED				



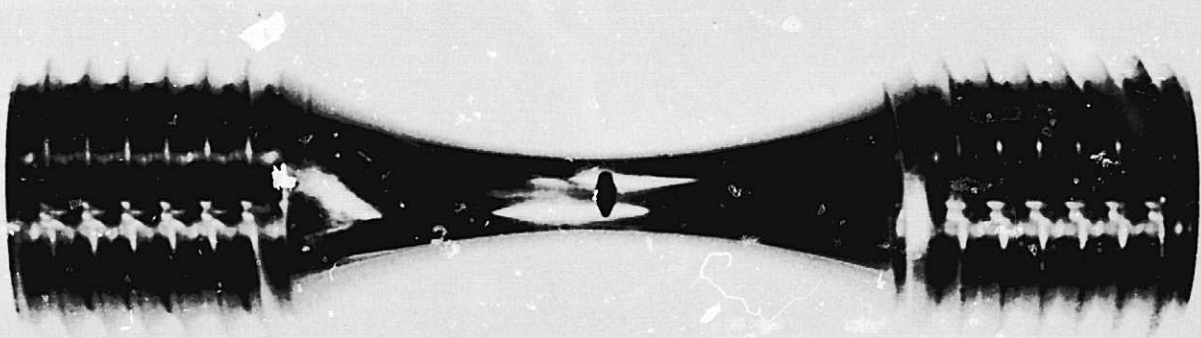
NOTES

1. A surfaces to be parallel within .001
2. A surfaces to be perpendicular to the center line of specimen within .0005 FIR
3. Contoured portion of specimen shall have a 16 finish and fine finish shall be in the axial direction, using low stress or polishing operation
4. All diameters shall be concentric within .001 FIR
5. Each specimen shall be individually packaged to prevent damage to the finished surfaces.
6. 32 finish all over, except as noted.

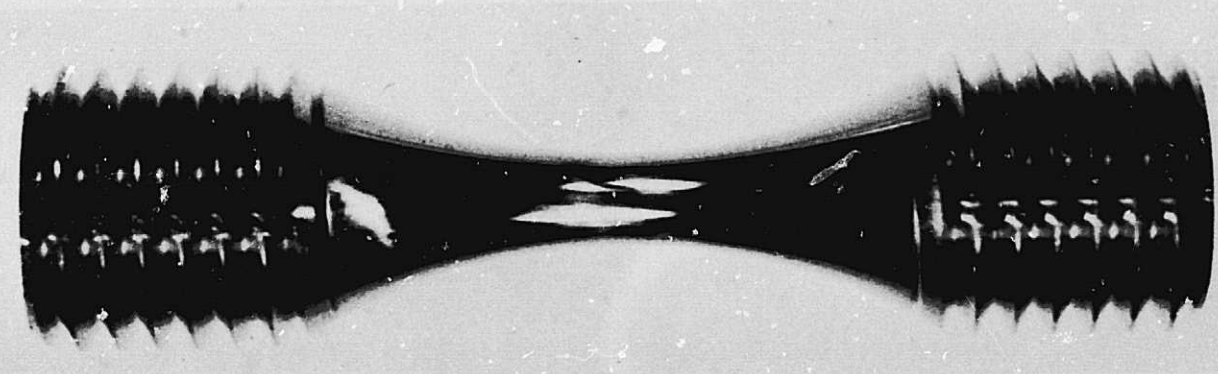
Figure 3 - LOW CYCLE FATIGUE SPECIMEN

(NOTCHED;  $K_t = 2$ )

MTI-1014



NOTCHED BAR  
( $K_T = 2$ )



SMOOTH BAR

Figure 4- Photograph of smooth-bar and notched-bar specimens.

#### IV - TEST EQUIPMENT

A closed-loop, servo-controlled, hydraulically-actuated fatigue machine (see Figure 5) was employed in this program. This machine was equipped with the necessary recorders to provide continuous readouts of the desired test information.

A block diagram of the type of test machine used is presented in Figure 6. The programmer is a precision solid-state device capable of furnishing all of the required waveform signals necessary to provide the strain or stress values demanded in the test. This signal is compared in the summing network with the strain or stress values actually present at the specimen at any instant of time. Any deviation from the required parameter is sensed by the servo-controller which supplies a correction current signal to the servo-valve which provides the correct hydraulic flow and pressure to the hydraulic actuator. The actuator in turn imparts the necessary displacement and force through the load cell to the specimen. The diametral displacement of the specimen in the gage section is sensed by the extensometer and the motion is imparted to the LVDT (Linear variable displacement transducer) which supplies an electrical signal to the analog computer. The analog computer accepts the instantaneous diametral strain and axial force signals and operates upon them to provide signals representing all of the strain and stress components of interest. Any one of these can be selected for comparison with the programmer signal.

Manufacturer and nomenclature of the various components of the fatigue machines are as follows:

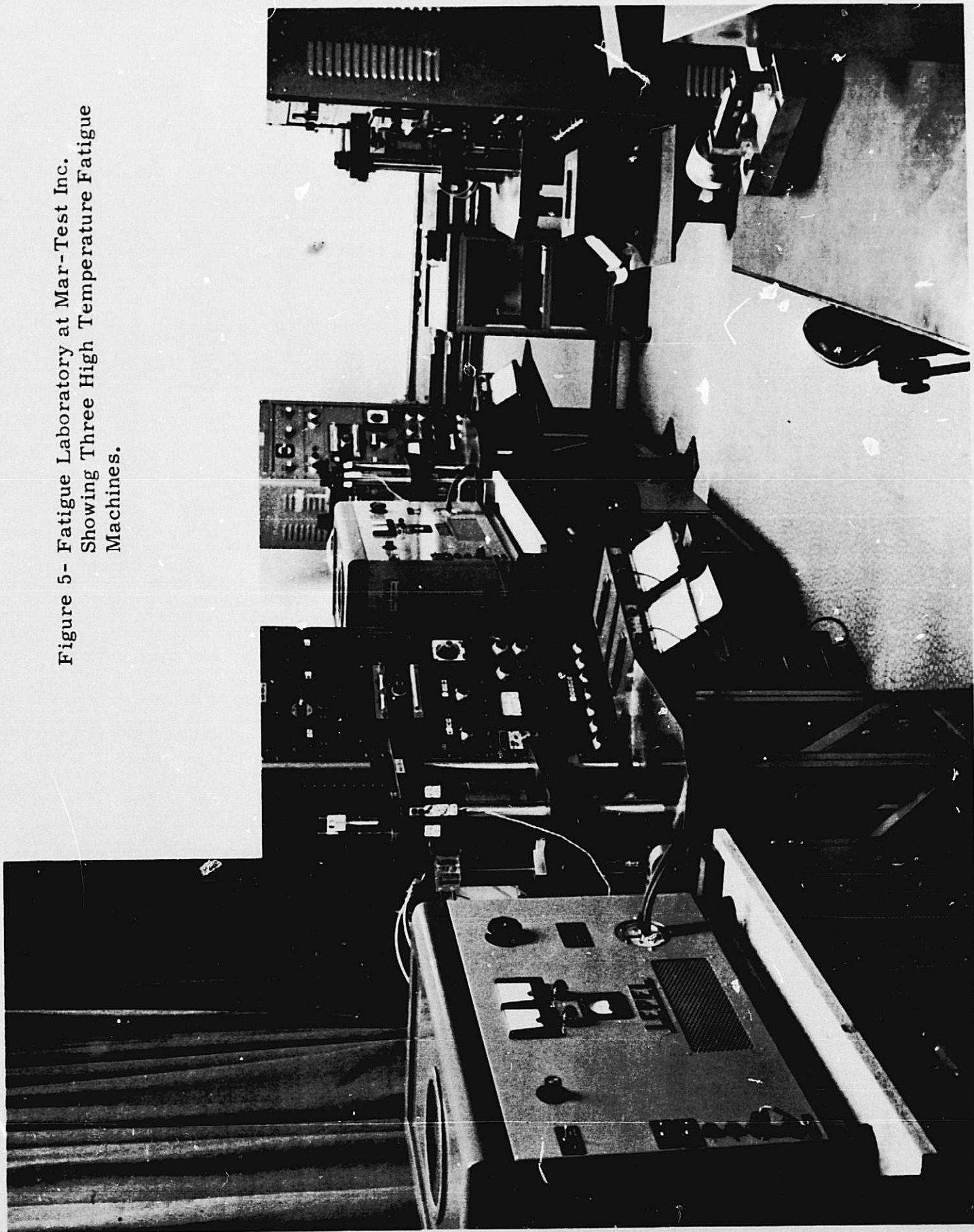
1. Programmer - designed and built by Mar-Test Inc.
2. Servo-controller - designed and built by Mar-Test Inc.
3. Actuator - Universal Fluid Dynamics, Type MDF5-H-BR
4. Servo-valve - Moog, Model 76-101
5. Hydraulic System - Racine, Model PSV-SS0-20GRS
6. Load Cell - Strainert, Model FFL15U-2SP (K)
7. Induction Generator - Lepel, Model T-2, 5-1-KC-J-BW
8. Extensometer - designed and built by Mar-Test Inc.  
to measure diametral strain
9. LVDT - ATC, Model 6234A05B01XX
10. Analog Strain Computer - designed and built by Mar-Test Inc.
11. Load Frame and Fixtures - designed and built by Mar-Test Inc.

Each fatigue machine consists of a sturdy three-column support system connecting two fixed, horizontal platens. A movable platen operates between the fixed platens and is hydraulically actuated to provide the desired cyclic motion. The movable platen contains three close-tolerance bushings which slide on the chrome-plated support columns to impart extreme rigidity and precise alignment to the system.

The diametral strain at the minimum diameter point of the specimen is measured using a specially constructed diametral extensometer. This device was fabricated from low thermal expansion materials (quartz and invar) to minimize the effects



Figure 5- Fatigue Laboratory at Mar-Test Inc.  
Showing Three High Temperature Fatigue  
Machines.



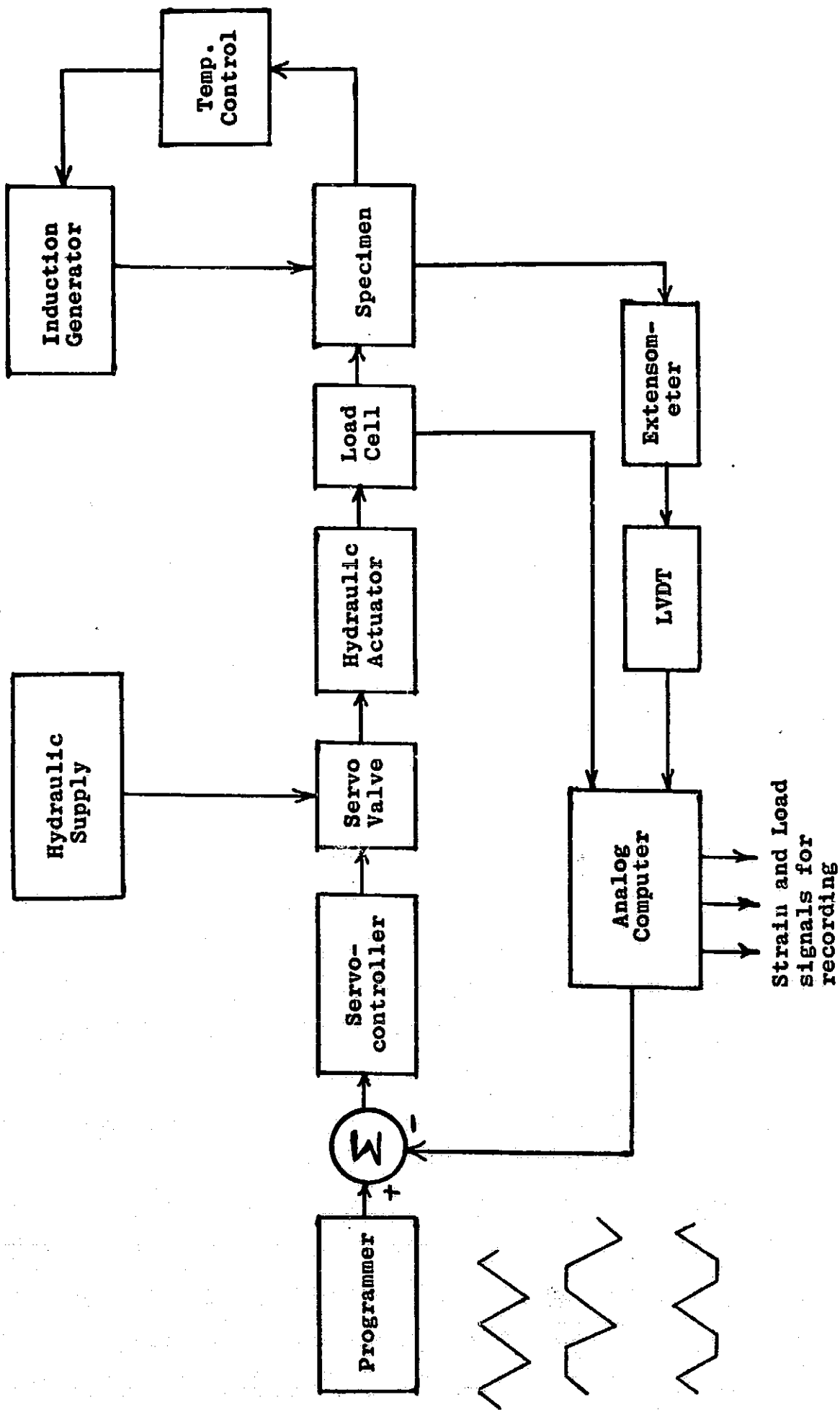


Figure 4- Schematic of components in fatigue testing machine.

of room temperature changes on extensometer output. Each extensometer is calibrated prior to use by employing a special calibration fixture. Each device is supported horizontally (that is, in the actual use position) with the extensometer knife edges touching a 0.25 inch diameter split pin. One of the pin halves is fixed and the other is displaced horizontally to simulate a diameter increase. This motion is controlled by the rotation of the barrel of a special micrometer (calibrated against NBS standard). In this way the extensometer is calibrated to within 10 microinches. With this type of calibration and a knowledge of the stability and accuracy of the electronic components of the system a reasonable estimate of the accuracy of the strain control system is 60 microinches per inch in terms of axial strain range.

Before any tests are made each load cell is calibrated in position by placing a calibrated (NBS) Ring-Force Gauge (Morehouse Instrument Co., Model 5 BT, 5000 lbs capacity with an accuracy to 0.2 percent) in the specimen position in the load train. As the actuator is caused to apply a load the output of the load cell is plotted against the load indicated by the calibrated Ring-Force Gauge. This calibration is performed at frequent intervals to insure accurate stress measurements during the testing program.

Each fatigue machine has its own control console which functions to supply the very precise control features which are so essential to the performance of meaningful fatigue tests. In addition to housing the temperature controller and an elapsed time indicator each control console contains:

- a) a calibration panel which also provides means for automatic or manual control of the hydraulic solenoid and power for auxiliary equipment such as the induction generator and recorders;
- b) a programmer which provides the required demand signal waveform for the test;
- c) an analog strain computer which generates the load and strain components for recording and control purposes;
- d) a servo-controller which compares the programmer supplied demand signal and the computer supplied feedback signal and generates the proper control current for the servo-valve; a meter relay circuit operates in conjunction with the servo-controller to provide the means for shutting down the system when the specimen fails.

One of the important precautionary features of the Mar-Test fatigue machines is the incorporation of a manually operated by-pass valve across the hydraulic actuator. With this valve open the test specimen cannot be exposed to any inadvertent load transients during start-up. The hydraulic solenoid valve can be energized with this valve open and the load transients frequently encountered in test start-up can be eliminated. Once

the solenoid valve is opened the by-pass valve can be closed slowly to bring the system under control. During this operation the load trace is monitored so that a smooth transfer is effected and all load transients are eliminated.

## V. - TEST PROCEDURES

### A. Low-Cycle Fatigue

The closed-loop, servo-controlled low-cycle fatigue machine employed in this study was fitted with a specially constructed containment vessel to allow testing in a protective environment. This cylindrical chamber was fabricated from 2-inch diameter pyrex tubing and was inserted between the holding fixtures. This small-volume enclosure (about 170cm<sup>3</sup>) facilitated system purging and allowed the desired protective gas purity levels to be maintained. Neoprene low-force bellows at the top and bottom connected the chamber to the holding fixtures and permitted the normal longitudinal motion of the specimen during cyclic loading. Side-arms on the pyrex containment vessel provided access for the extensometer arms and a special flexible joint provided an effective seal without influencing the strain measurement. Thermocouple lead-throughs were provided near the lower platen so that the thermocouple leads could be routed from within the enclosure to the temperature control system. Specimen heating was effected by an induction coil wound around the external surface of the cylindrical containment chamber (see Figure 1).

All the low-cycle fatigue tests in this program were performed using the specimen configuration shown in Figure 2. Such specimens were held in specially designed threaded adaptors to provide an integral assembly that allowed the adaptor to be heated inductively along with the specimen itself. Large mating surfaces were provided between the specimen and the adaptors to minimize the temperature gradient between them. This approach proved to be quite successful and test temperatures to 593°C (1100°F) were achieved quite readily. It was also shown that a very flat longitudinal temperature profile was obtained.

Test temperatures were measured using a chromel-alumel thermocouple clamped tightly against the specimen in the region where the contoured portion of the specimen meets the threaded portion. This approach was found to be very reliable and very easy to apply. It also provided more accurate temperature control particularly in thermal-mechanical tests where fast response to gage section temperature changes is essential.

Because of the temperature uniformity in the specimen-adaptor assembly a special precaution must be taken to avoid failure in the threaded portion of the specimen. This involves the provision of a large specimen diameter in the grip region compared to the diameter at the specimen midpoint. This was also

sufficient to avoid plastic deformation at the specimen-adaptor contact point and therefore to prevent backlash and alignment changes during strain cycling.

A fully instrumented test specimen-adaptor assembly was mounted in the holding fixture of the fatigue machine using a split collet type of assembly and a special leveling device was employed to assure that the specimen was installed perpendicular to the platens. A flat load cell (see previous section) in series with the specimen was used to measure the load applied to the specimen throughout the test.

Once the specimen was installed within the containment vessel the system was purged using a high flow rate of high purity argon (see below for inert gas specifications) for 30 minutes. This established the desired purity level within the test chamber. The inert gas flow rate was then lowered to a few  $\text{cm}^3/\text{min}$  and maintained at this level throughout the test.

Before any tests were initiated the analog strain computer was calibrated by making use of the specimen cross-sectional area (A) and the value for Young's modulus (E) at the intended test temperature. Modulus values for the two alloys tested were determined in separate tests. The values of A and E were used as shown in the block diagram in Figure 7 to generate axial strain values corresponding to measured values of diametral strain and force. This diagram provides an aid to an understanding of the computer calibration procedure which is based on using the values of A and E and adjusting the compliance control to establish the following equality:

$$AE = F/\epsilon_e$$

Prior to heating a specimen to the desired test temperature the system was placed in force control. This automatically kept the force at zero by gradually lowering the movable platen to account for the thermal expansion of the specimen as the temperature was increased. When test temperature was obtained the analog strain computer was employed to yield a value for Poisson's ratio. The specimen was cycled elastically so that the actual plastic strain,  $\Delta\epsilon_p$ , was zero and the value of Poisson's ratio could be obtained by the ratio of the diametral to axial strain; thus:

$$\nu_e = -\frac{\epsilon_d}{\epsilon_e}$$

The  $\nu_e$  control on the computer was then adjusted to force the computer value of  $\Delta\epsilon_p$  to zero. At this point the above relations were satisfied and the correct value of  $\nu_e$  was indicated

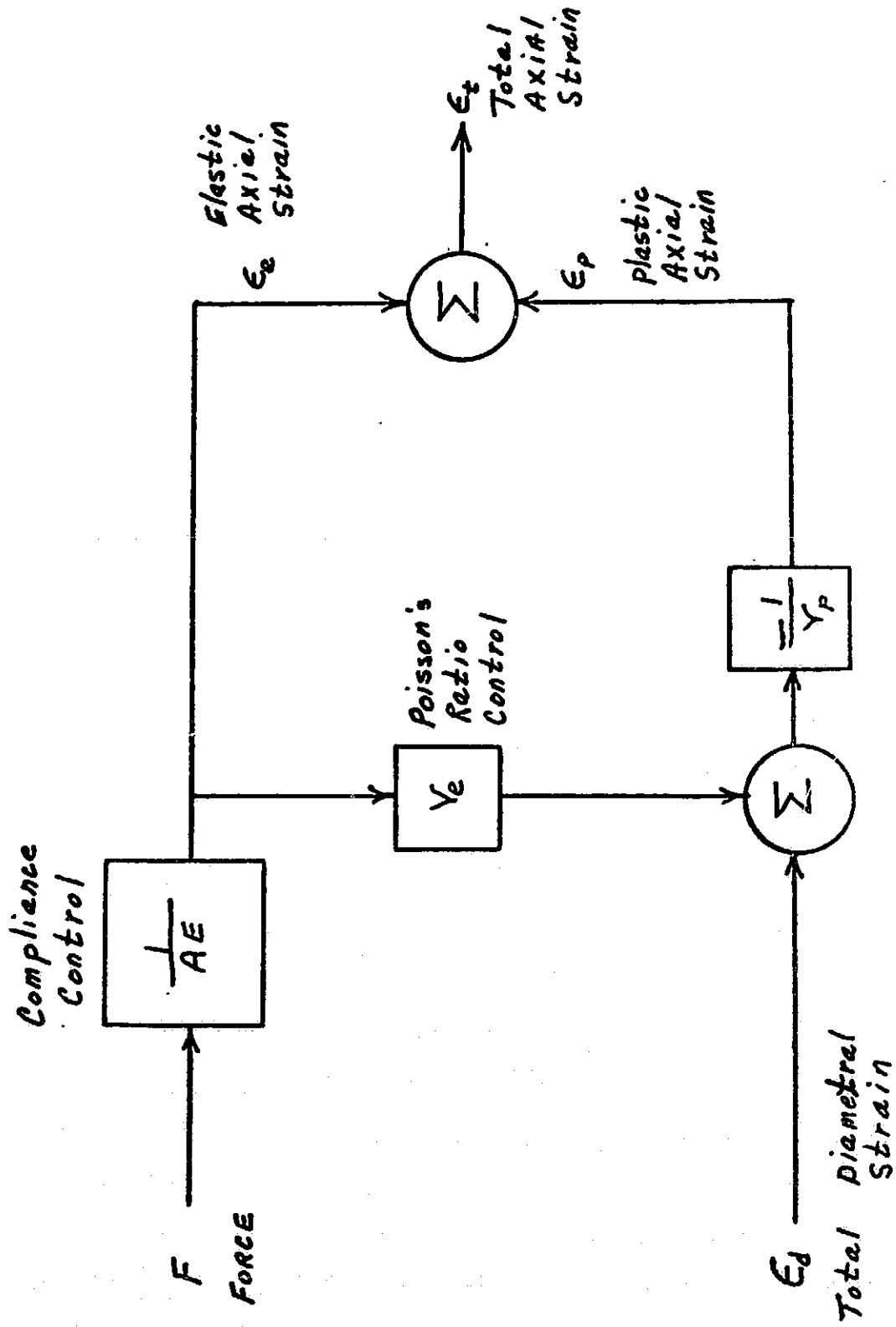


Figure 7- Block Diagram of Strain Computer

on a potentiometer turns-counting dial on the computer panel (the value for Poisson's ratio, plastic, was set internally to 0.5 in accordance with constant volume deformation conditions associated with plastic deformation). At this point the computer was calibrated and furnished a correct axial strain signal for recording and control purposes.

With the computer calibration complete the test was ready to begin. Two recorders were connected to the console, one to monitor load and the other to monitor the total axial strain. The system was placed in automatic control and the strain was gradually increased to the desired level. This gradual increase to the desired strain level requires 5 or 6 cycles and avoids specimen damage due to "overshooting" the strain range which can occur if an attempt is made to impose the desired strain level on the first loading cycle. When the desired strain range was reached the test conditions were kept constant until fracture occurred. Hysteresis loops were recorded on an x-y recorder during the first few cycles and at frequent intervals thereafter. In addition, a continuous recording was made of the applied load and the associated plastic strain. When the specimen fractured, the shut-down circuit automatically de-energized the entire testing system including the induction generator, the hydraulic ram, the timing device and the recorders. However, the protective environment system remained functional until the specimen cooled to room temperature.

High purity (guaranteed 99.999% purity or better) argon gas was employed as the protective environment for the first few tests in the Task 1 portion of this program. It was found, however, that more protection was afforded by the use of a slightly reducing environment which consisted of this same high purity argon gas with an addition of 1000 ppm of hydrogen. This latter environment provided completely satisfactory results for all the high temperature tests of the zirconium-copper alloy specimens. Some indication of the effectiveness of this environment in these tests is provided by the fact that some of the Task 2 tests involved durations close to 60 hours and yet the specimens had a clean and bright appearance at the end of the test. It was not found necessary to employ the tantalum "getter" foil used in some of the Task 1 evaluations.

### B. Short-Term Tensile

Measurements of short-term tensile behavior were made using the same hydraulically-actuated, servo-controlled fatigue machines employed in the low-cycle fatigue evaluations. Furthermore, the same specimen design was employed and the specimen preparation, test environment, installation and instrumentation procedures were identical to those employed in the fatigue tests. These short-term tensile tests were performed using a diametral extensometer and the true diametral strain rate was kept constant at the specified value (the corresponding axial strain rate was about twice this value).



For each test a strip chart recording was made of the measured diametral strain as a function of time and, in addition, an x-y recording was made of the load versus diametral strain. These traces provide test information from the instant of load application all the way to fracture.

### C. Thermal-Mechanical Testing

Combined thermal-mechanical tests were conducted using the same equipment employed in the previous fatigue and tensile portions of this program. In those thermal-mechanical tests, however, it was necessary to cycle the specimen temperature between prescribed limits while the mechanical strain was being cycled and controlled in accordance with the usual procedure followed in an isothermal low-cycle fatigue test.

The "Thermal-Mechanical Circuit" employed in conjunction with the testing machine provided the necessary command signals and signal conditioning required for these special tests. The functions provided by this circuit are listed and described in the following paragraphs.

#### 1. Isolation of the Mechanical Strain

The output of the strain extensometer, in these kinds of tests, consists of the algebraic sum of two separate displacement signals. One signal is caused by the temperature change and under conditions of no constraint would simply be a measurement of the thermal expansion or contraction of the specimen. The other signal is associated with a stress in the specimen, whether this stress is caused by a directly applied or resultant force and is referred to as the mechanical strain. Isolation of this latter component can be effected by subtracting a specially generated analog of the thermal component from the total extensometer signal. This thermal correction signal is obtained from a function generator circuit which uses the specimen temperature as an input. Before every test, final adjustments are made and a measure of the accuracy of the subtraction technique is evaluated. To do this, the specimen is thermally cycled a few times under zero load conditions while the "mechanical strain" signal is adjusted to as small a level as possible. The extensometer signal corrected for this thermal component is then used as an input to the analog strain computer.

#### 2. Generation of the Temperature Command Signal

The Thermal-Mechanical Circuit also produces a triangular waveform command signal for the temperature controller. The mean level as well as the amplitude are adjustable and the frequency is synchronized to that of the strain command signal. In addition, the phase of this signal can be changed by  $180^\circ$  so that the peak temperature can be made to correspond to either the peak tension or the peak compression level of the strain cycle. Figure 8 is a simplified block diagram of the Thermal-Mechanical Circuit, showing the input and output signals.

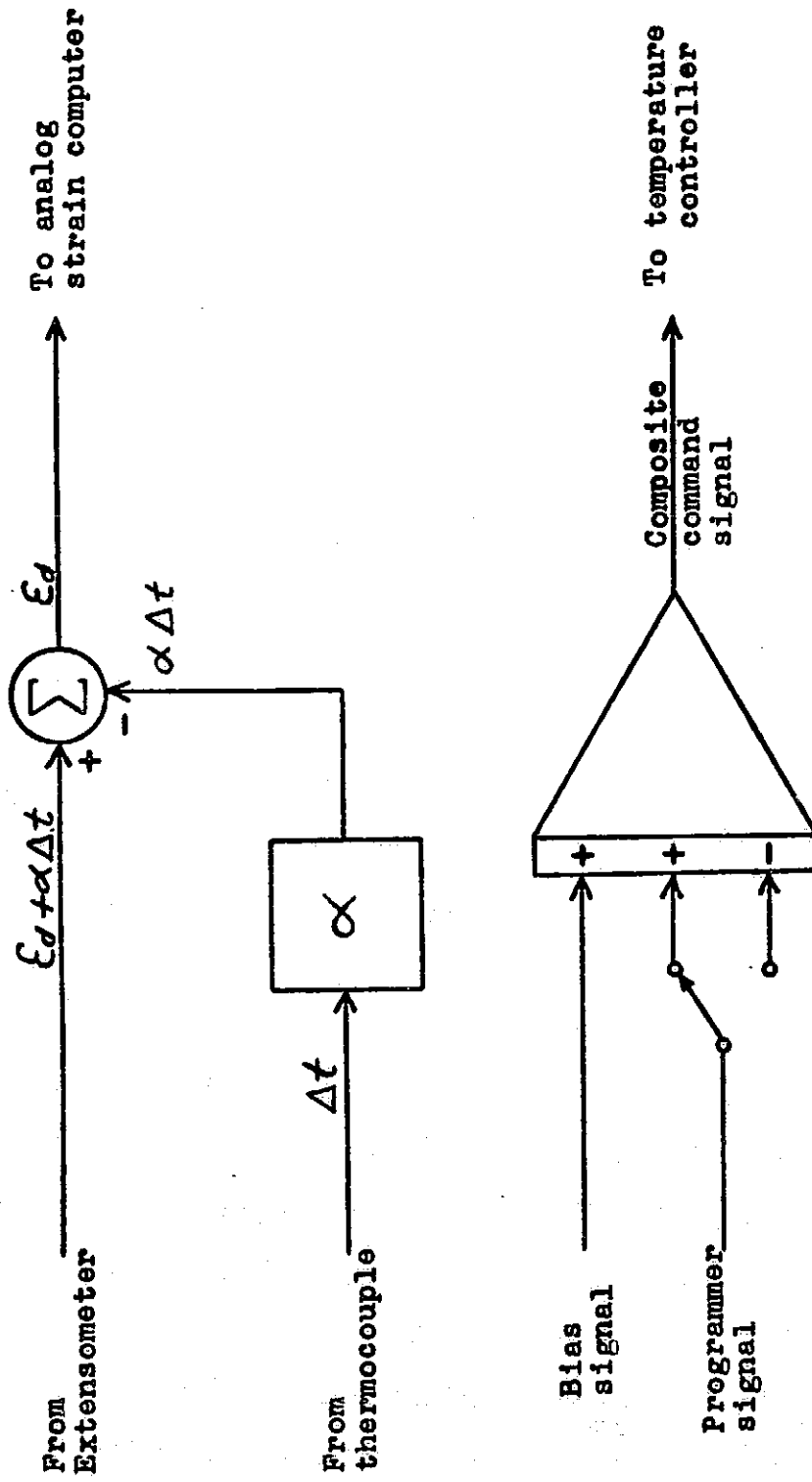


Figure 8- Simplified block diagram of Thermal-Mechanical Circuit.

For all of the thermal-mechanical tests, the analog strain computer was calibrated by using the 538°C values for E (modulus of elasticity) and  $\nu_e$  (Poisson's Ratio) since no provisions exist for dynamic adjustment of these material constants as a function of changing temperature. Primarily because of the large amount of plastic strain in these tests however, this results in only a slight error (approximately 1%) in the computation of the axial strain at 260°C.

Some difficulty was encountered in obtaining the desired thermal response of the specimen in these tests. Because of the high thermal and electrical conductivity of copper all previous testing utilized heat resistant specimen adapters in the load train to facilitate heating to 538°C. Unfortunately, however, these same adapters impede cooling the specimen in a thermal-mechanical test. It was necessary therefore to use higher conductivity adapters to enhance the cooling rate even though this required more power from the induction generator when heating. The required compromise resulted in a linear and symmetrical waveform having a period of about 13 minutes. All of the thermal-mechanical tests, therefore, employed a frequency of about 4.5 cycles per hour.

## VI - TEST RESULTS AND DISCUSSION OF RESULTS

### A) Short-Term Tensile

Short-term tensile tests of the R-20 alloy (second lot of zirconium-copper, 1/2 Hard, alloy) were performed in duplicate at room temperature and at 538°C using a strain rate of  $2 \times 10^{-3} \text{ sec}^{-1}$ . The results obtained in these evaluations are presented in Table 2. A study of these results indicates noticeably lower (about 20%) yield and ultimate strengths compared to those exhibited by the R-2 alloy. These differences are illustrated in Figure 9. Reduction in area values are essentially identical for the R-2 and R-20 materials at room temperature and just slightly higher for the R-20 material at 538°C.

### B) Low-Cycle Fatigue

#### 1) Smooth Versus Notched Behavior

Room temperature low-cycle fatigue tests of the R-2 alloy were performed in air in axial strain control to provide a comparison of smooth bar (see Figure 2) and notched bar (see Figure 3) behavior. A summary of the results obtained in these tests is presented in Tables 3 and 4. A very slight initial hardening followed by cyclic softening was observed in each test and a comparison of the stress range at start and at half-life is presented in Figure 10 based on smooth bar results. The half-life stress range is seen to be some 20% lower than that at start. The stress range at start was noted to be very close to the monotonic stress-strain behavior observed in the Task 1 tests.

A comparison of the fatigue life for the smooth and notched bars is presented in Figure 11. It can be seen that for a given strain range the ratio of smooth-bar to notched-bar fatigue life is constant at about 6.0 over the range of reported data. It can also be noted that for a given fatigue life the ratio of the strain range for the smooth bar to the strain range for the notched bar is approximately equal to a factor of 2.0 which corresponds to the theoretical elastic stress(strain) concentration factor of 2.0 for the notched configuration employed in these tests. It is also interesting to note that these smooth bar data at room temperature are essentially identical to those obtained at 538°C in Task 1 ( see comparison of data in Figure 13).

A plot of the fatigue life versus plastic strain range for the R-2 alloy(smooth bar data) at room temperature is shown in Figure 12. These results define a fairly linear relation and a slope of approximately -0.6 is indicated.

#### 2) Low-Cycle Fatigue Data for R-20 Alloy

These tests represent an evaluation of the low-cycle fatigue characteristics of a second lot of 1/2 Hard, zirconium-copper alloy(see Table 1). Tests were performed in accordance

Table 2 - Short-Term Tensile Properties of R-20 (Zr-Cu, 1/2 Hard) Alloy Measured in Argon, (room temperature tests were performed in air)

Diametral Extensometer		Hourglass-Shaped Specimens			
Spec. No.	Temp., °C	Strain Rate, sec <sup>-1</sup>	0.2% Offset Yield Strength, MN/m <sup>2</sup>	Ultimate Tensile Strength, MN/m <sup>2</sup>	Reduction in Area %
R-20-7	RT	$2 \times 10^{-3}$	295	306	81
R-20-8	RT	$2 \times 10^{-3}$	302.7	314	79
R-20-9	538	$2 \times 10^{-3}$	135	140.7	90
R-20-10	538	$2 \times 10^{-3}$	133	136	91

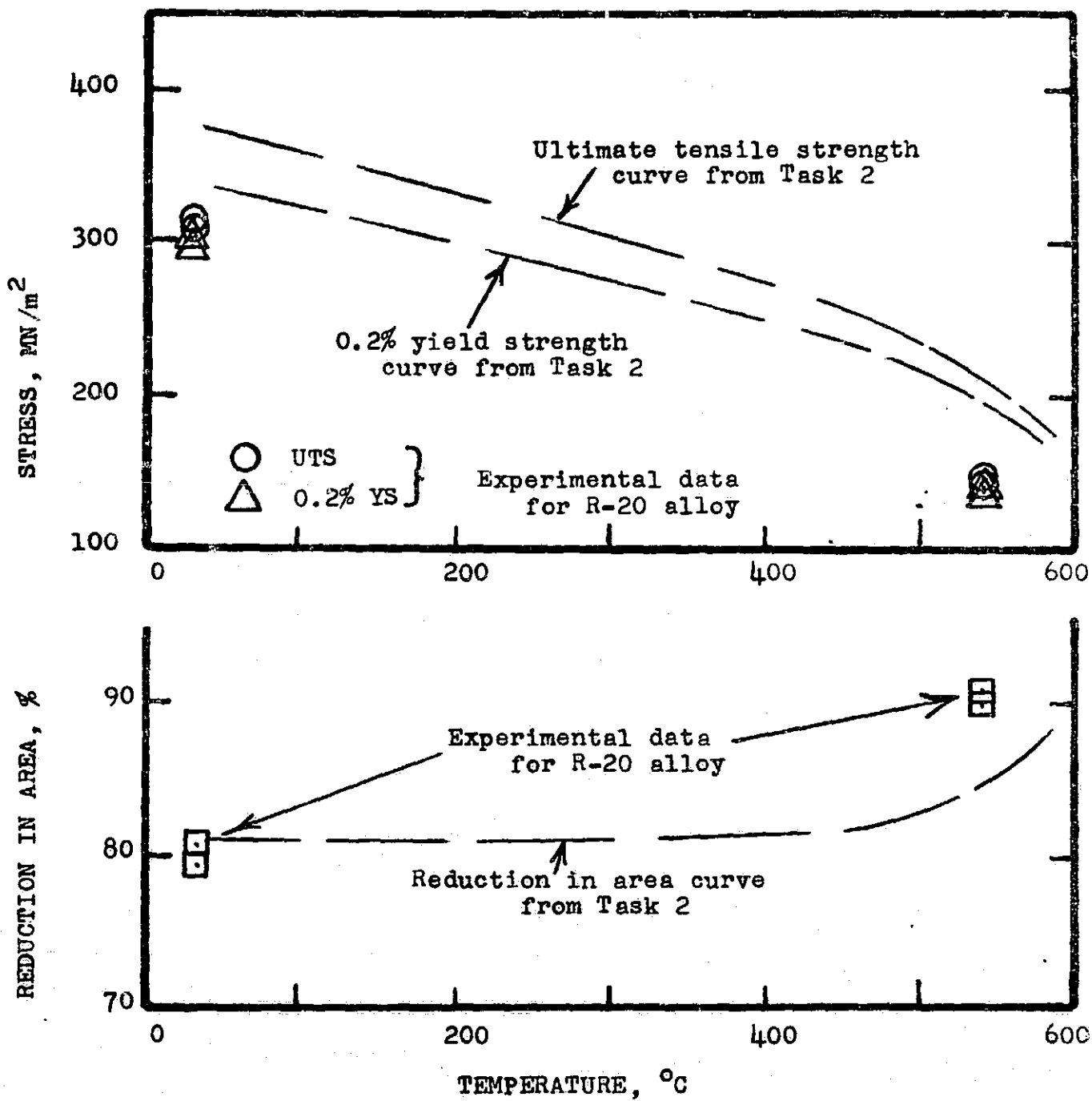



Figure 9- Comparison of short-term tensile properties of R-20, zirconium-copper alloy, with data for R-2 alloy reported in Task 2.

Table 3 - Low-Cycle Fatigue Test Results Obtained in Air at Room Temperature (smooth bar) Using a Strain Rate of  $5 \times 10^{-3}$  sec<sup>-1</sup>

Spec. No.	Poisson's Ratio	Total Strain Range, %	Freq. cpm	Stress Range at Start, MN/m <sup>2</sup>	at $N_f/2$			$N_f$ , Cycles to Failure	Remarks
					$\Delta \epsilon_p$ %	$\Delta \epsilon_e$ %	$\Delta \sigma$ MN/m <sup>2</sup>		
R-2-17	0.365	3.0	5	702	2.49	0.51	587	696	 Slight initial hardening followed by softening
R-2-51	0.36	2.5	6	674	2.043	0.457	527	1102	
R-2-52	0.36	1.6	9.38	667	1.172	0.428	493	2780	
R-2-53	0.36	4.0	3.75	716	3.50	0.50	576	425	
R-2-54	0.36	1.4	10.71	667	0.98	0.42	485	3283	

Axial Strain Control  
 A-ratio of infinity  
 $E = 115.1 \times 10^3$  MN/m<sup>2</sup>

R-2-Series  
 Zirconium-Copper; 1/2 Hard

Table 4 - Low-Cycle Fatigue Test Results Obtained in Air at Room Temperature  
(notched bar) Using a Strain Rate of  $5 \times 10^{-3} \text{ sec}^{-1}$

Spec. No.	Poisson's Ratio	Total Strain Range, %	Freq. cpm	Stress Range at Start, $\text{MN/m}^2$	at $N_f/2$			$N_f$ , Cycles to Failure	Remarks
					$\Delta \epsilon_p$ %	$\Delta \epsilon_e$ %	$\Delta \sigma$ $\text{MN/m}^2$		
R-2-55	0.35	3.0	5	703	2.5	0.50	576	↑ Slight initial hardening followed by softening ↓	
R-2-56	0.35	1.4	10.71	662	0.95	0.45	527		
R-2-57	0.36	0.9	10 <sup>a</sup>	634	0.49	0.41	469		
R-2-58	0.35	2.0	7.5	689	1.52	0.48	552		
R-2-59	0.35	0.7	12.86 <sup>a</sup>	593	0.34	0.36	420		

Axial Strain Control  
A-ratio of infinity  
 $E = 115.1 \times 10^3 \text{ MN/m}^2$

Series R-2  
Zirconium-Copper; 1/2 Hard

a) strain rate of  $3 \times 10^{-3} \text{ sec}^{-1}$



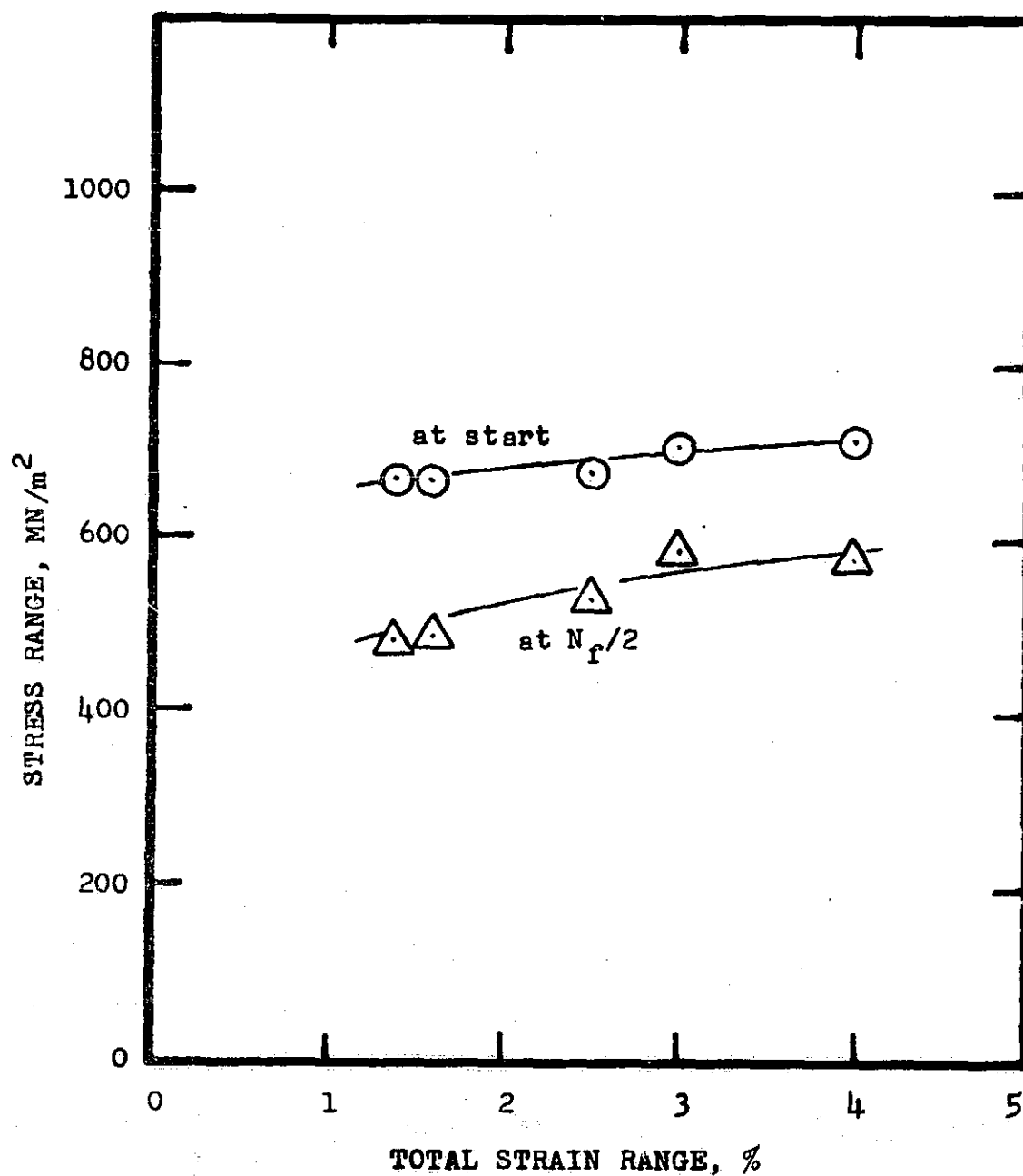


Figure 10- Stress range versus strain range data for R-2 alloy tested in air at room temperature in axial strain control.

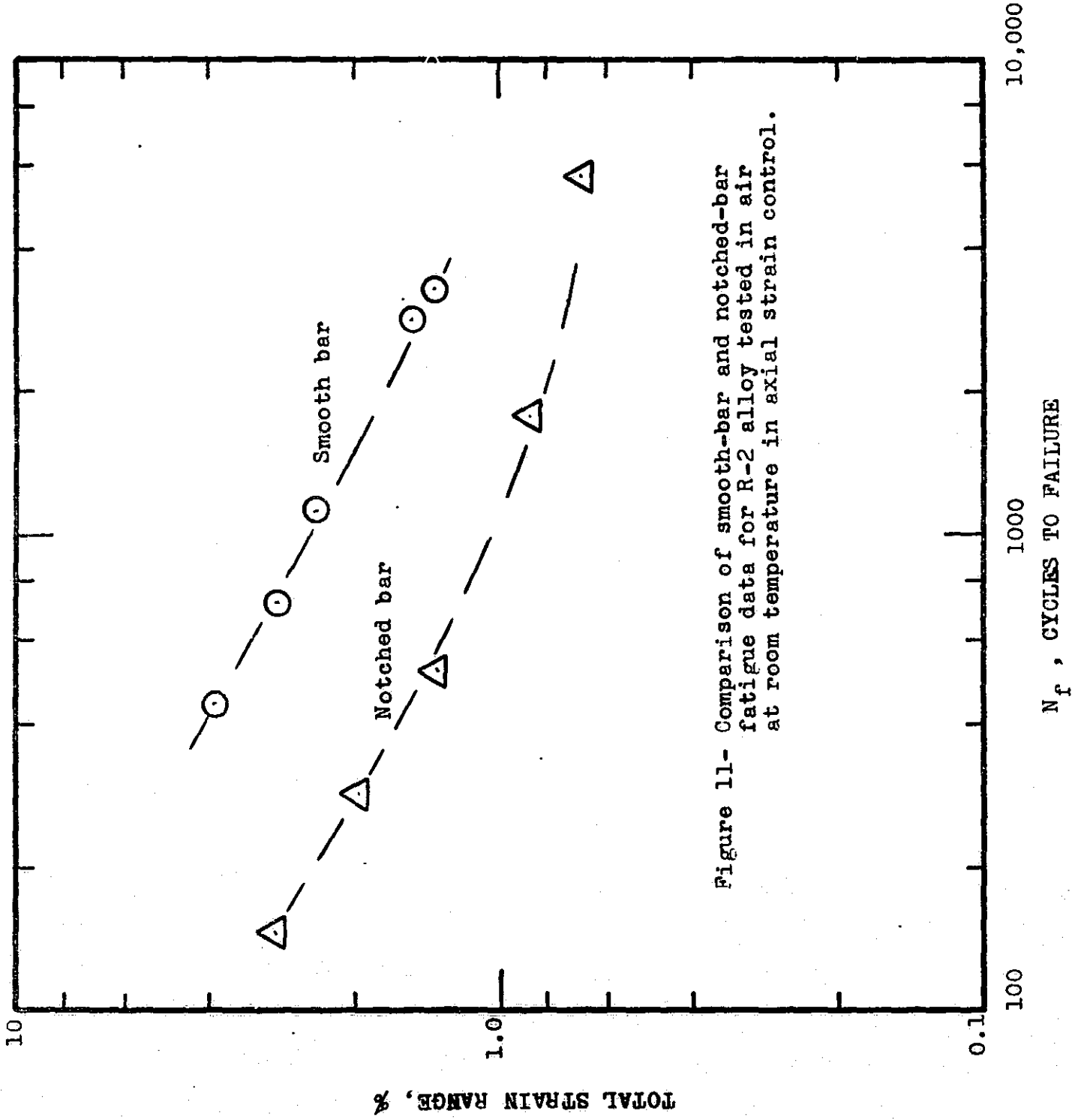


Figure 11- Comparison of smooth-bar and notched-bar fatigue data for R-2 alloy tested in air at room temperature in axial strain control.

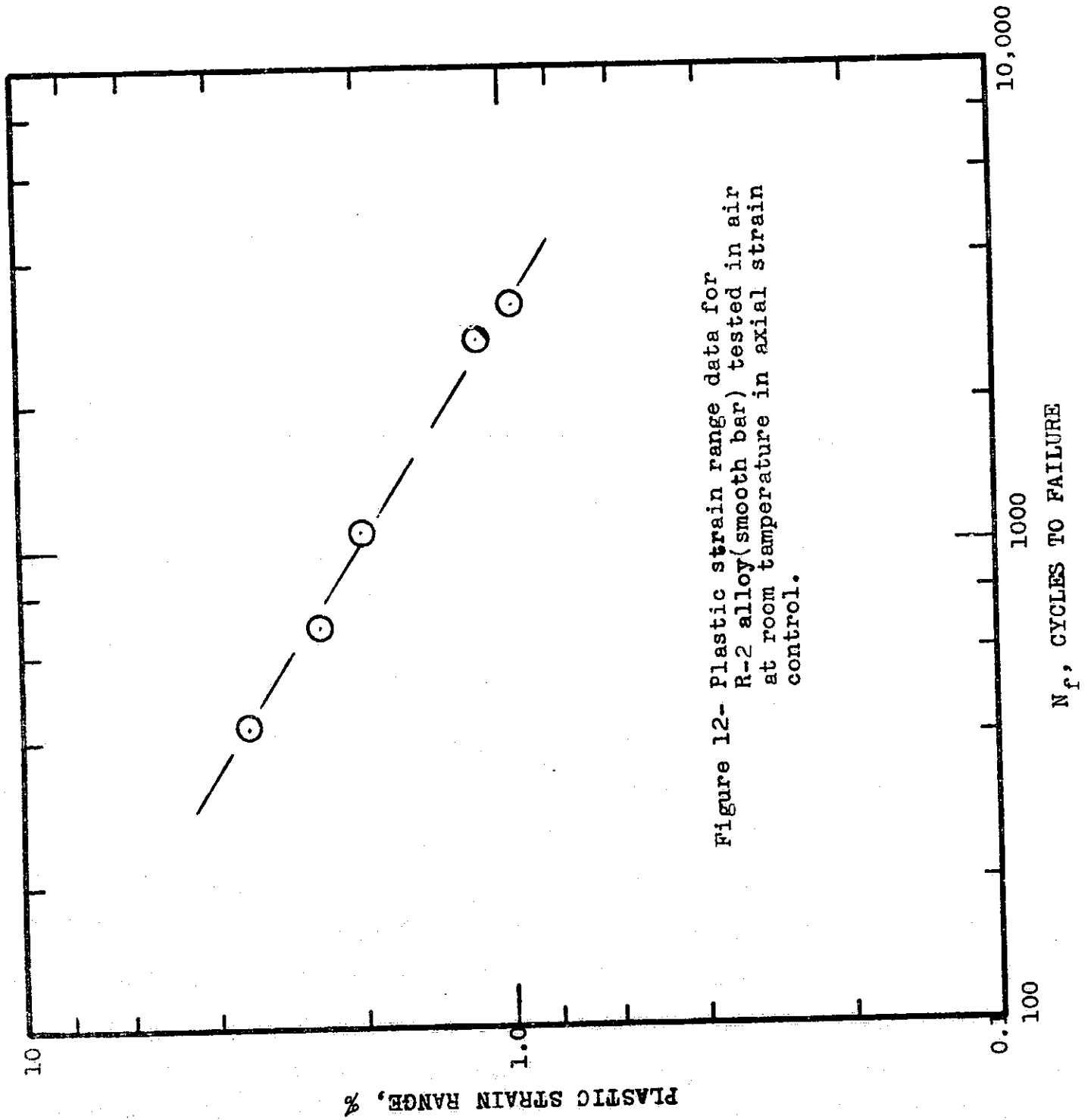
10,000

1000

100

N<sub>f</sub>, CYCLES TO FAILURE

TOTAL STRAIN RANGE, %



with the test matrix followed in Task 1 (see NASA CR-121259) to define the fatigue life over the range from about 300 to 3000 cycles at 538°C, a strain rate of  $2 \times 10^{-3} \text{ sec}^{-1}$ , and an A-ratio of infinity in axial strain control. A summary of the test results obtained in these evaluations of the R-20 material is given in Table 5. These data define a fatigue behavior which is essentially identical to that exhibited by the R-2 alloy in similar tests performed in the Task 1 portion of this program (see NASA CR-121259). A comparison of the fatigue data for these two lots of the zirconium-copper, 1/2 Hard, alloy tested in argon at 538°C is shown in Figure 13. This comparison substantiates the above statement that essentially identical fatigue behavior seems to be exhibited although there does appear to be some indication that longer fatigue life is attained by the R-20 material in the strain range regime close to 1.5%.

Also shown in Figure 13 are the smooth-bar fatigue data for the R-2 material tested at room temperature (from Figure 11). These data also appear to be essentially identical to the R-2 and R-20 results at 538°C to suggest the existence of little to no temperature effect on the low-cycle fatigue behavior for the zirconium-copper, 1/2 Hard, alloy. This observation extends the conclusion made in the Task 2 report (NASA CR-121260) that the fatigue behavior of the R-2 alloy was unaffected by temperature over the temperature range from 482° to 593°C.

### 3) Hold-Time Effects

Some additional hold-time tests of the R-2 alloy in argon at 538°C were performed to extend the hold-time information described in the Task 2 report. A hold time of 300 seconds was selected and this was imposed in tension only, compression only, and in both tension and compression. The results obtained in this study are summarized in Table 6 where it is indicated that a certain dimensional instability was involved. This phenomenon was discussed in the Task 2 report of R-2 testing where it was observed that the effect became particularly severe in the longer-term tests. This same phenomenon was noted in the tests summarized in Table 6 and, as before, the effect was most pronounced in the longer term tests. It was also noted in this program that the phenomenon termed "barrelling" was particularly severe in those tests involving a hold period in compression only whereas a "double-necking" phenomenon was observed in those tests involving a hold time in tension only. This "necking" phenomenon was characterized by the formation of "necked down" portions of the specimen at points above and below the extensometer location. Failure occurred at one of the "necked down" locations. While "barrelling" has been observed and described before this appears to be the first known observation of a "double necking" phenomenon in low-cycle fatigue testing. It is difficult to explain this type of specimen instability at this time.

Mention is made of this dimensional instability problem

Table 5 - Low-Cycle Fatigue Test Results Obtained in Argon at 538°C Using a Strain Rate of $2 \times 10^{-3} \text{ sec}^{-1}$									
R-20 Series Zirconium-Copper; 1/2 Hard; Lot 2									
Spec. No.	Poisson's Ratio	Total Strain Range, %	Freq. cpm	Stress Range at Start, $\text{MN/m}^2$	at $N_f/2$			$N_f$ , Cycles to Failure	Remarks
					$\Delta \epsilon_p$ %	$\Delta \epsilon_e$ %	$\Delta \sigma$ $\text{MN/m}^2$		
R-20-1	0.36	5.0	1.2	269	4.87	0.13	105	390	softened
R-20-2	0.36	1.4	4.28	278	1.28	0.12	97.2	5,658	"
R-20-3	0.36	2.0	3	262	1.88	0.12	96.5	1,326	"
R-20-4	0.36	3.0	2	269	2.874	0.126	101.5	879	"
R-20-5	0.36	1.6	3.75	267	1.479	0.121	97.7	3,589	"
R-20-6	0.36	1.8	3.33	268	1.684	0.116	93.7	2,700	"

Axial Strain Control  
A-ratio of infinity  
 $E = 80.7 \times 10^3 \text{ MN/m}^2$

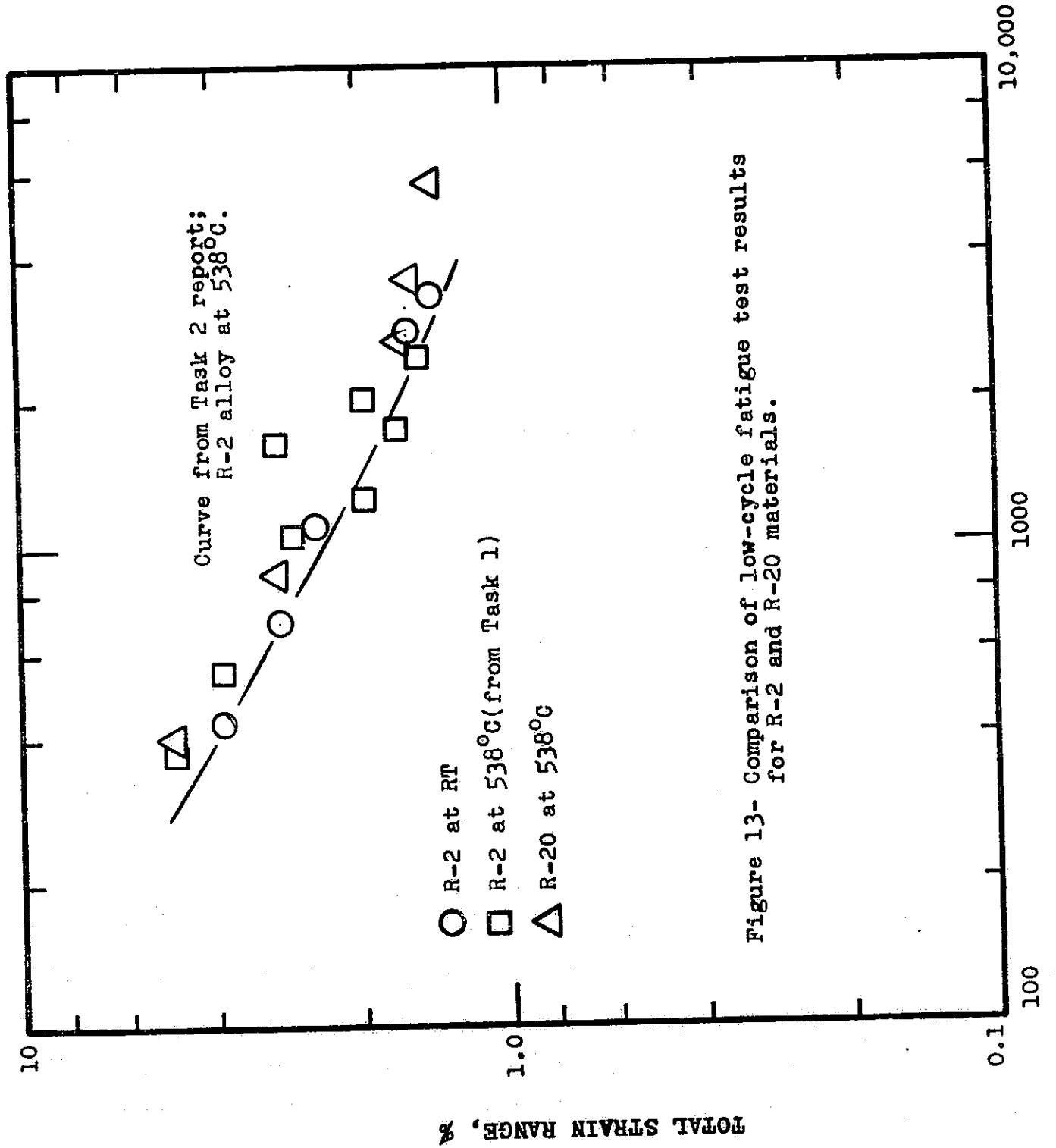


Figure 13- Comparison of low-cycle fatigue test results for R-2 and R-20 materials.

$N_f$ , CYCLES TO FAILURE

Table 6 - Low-Cycle Fatigue Results Obtained in Hold-Time Tests in Argon at 538°C Using  
a Ramp Strain Rate of  $2 \times 10^{-3} \text{ sec}^{-1}$

Spec. No.	Poisson's Ratio	Total Strain Range, %	Cycling Data		N <sub>f</sub> , cycles to failure	Remarks
			Ramp Time, Sec	Hold Time, Sec		
			R-2-67	0.36		
R-2-68	0.355	1.4	14	300, Tension	1156	softened; extensive necking outside of gage.
R-2-69	0.355	4.62	50	300, Compression	948	softened; extensive barrelling.
R-2-72	0.355	1.4	14	300, Compression	1224	softened; extensive barrelling.
R-2-73	0.35	5.0	50	300, Tension and compression	234	softened; some barrelling.

Axial Strain Control  
A - Ratio of Infinity  
E =  $80.7 \times 10^3 \text{ MN/m}^2$

R-2 Series  
Zirconium-Copper; 1/2 Hard

Table 6 - (contd) - Low-Cycle Fatigue Results Obtained in Hold-Time Tests in Argon at 538°C Using a Ramp Strain Rate of  $2 \times 10^{-3} \text{ sec}^{-1}$

Spec. No.	Stress Range at Start, MN/m <sup>2</sup>	at $N_f/2$						$R_\sigma$ Amount of Stress relaxation MN/m <sup>2</sup>	$\Delta \epsilon_p$ , %	$\Delta \epsilon_e$ %
		$\Delta \sigma$ MN/m <sup>2</sup>	$\sigma_t$ MN/m <sup>2</sup>	$\sigma_c$ MN/m <sup>2</sup>	$\sigma_f^*$ MN/m <sup>2</sup>	$\sigma_e$ MN/m <sup>2</sup>	$\sigma_f$ MN/m <sup>2</sup>			
R-2-67	338	126.9	61.4	65.5	24.1 T	37.3 T	4.90	0.111		
R-2-68	378	97.9	48.3	49.6	10.3 T	38.0 T	1.34	0.074		
R-2-69	330	120.7	59.3	61.4	30.3 C	31.1 C	4.56	0.111		
R-2-72	387	115.9	55.2	60.7	29.6 C	31.1 C	1.30	0.105		
R-2-73	347	124.1	60.3	63.8	22.8 T	37.5 T	4.99	0.068		

Axial Strain Control  
A - Ratio of infinity  
E =  $80.7 \times 10^3 \text{ MN/m}^2$

R-2 Series  
Zirconium-Copper; 1/2 Hard

\*T for tension and C for compression      \*\*Based on relaxed stress range



since the distortion of the specimen was so extensive that an accurate assessment of the hold-time effects might be difficult to obtain. For example, in the test of Spec. No. R-2-67 the 300-second hold period in tension only, at a strain range of 1.4% yielded essentially the same fatigue life reported in Task 2 for the 56-second hold period in tension at this same strain range. In other words, increasing the hold period duration from 56 to 300 seconds at a strain range of 1.4% led to virtually no further decrease in the fatigue life. While this saturation effect on fatigue life is possible it might not be completely correct in this instance because of the instability involved.

Another interesting point in Table 6 relates to the tests of Spec. Nos. R-2-68 and R-2-72. The fatigue life values of 1156 and 1224 cycles can be compared to values of 1947 and 3180 cycles reported in Task 2 for duplicate tests at this same strain range using a 56-second hold period in compression only. While the trend to lower fatigue life with increasing hold period duration is consistent the fact that a 300-second hold period leads to the same fatigue life whether it occurs in tension only or compression only, is subject to some question. Some further verification of this point is obviously in order.

A final observation involves the test of Spec. No. R-2-69. This fatigue life of 948 cycles is much greater than expected and there seems to be no reasonable explanation for this behavior. It is so much greater than that obtained in the continuously cycling tests that it cannot be viewed as a hold-time effect. The only reasonable explanation at the moment is that the barrelling which occurred interfered with the strain measurement and control. Some additional testing and analysis will have to be performed if this phenomenon is to be explained in detail.

A brief study was made of the relaxation behavior observed in each hold-time test. Because of the dimensional instability problem this study focused on the behavior in the early portion of the tests since it was felt that in this regime the specimen geometry was still unaltered and an accurate assessment of the relaxation characteristics could be obtained.

Relaxation curves (chosen from the first 20 cycles of the test) for the hold-time tests in Table 6 are presented in Figures 14 through 17. In Figure 14, relaxation curves for Cycle Nos. 5 and 20 are presented and reflect the cyclic softening that is taking place in this material. Despite the different stress values and the different amounts of stress relaxation ( $R_{\sigma}$ ) the ratio of  $R_{\sigma}$  to  $\sigma$  is essentially identical at 0.59 for each cycle. This same type of observation was made for the relaxation results reported in Task 2.

A comparison of tension and compression relaxation characteristics obtained in the 8th cycle of the test of Spec. R-2-73 is shown in Figure 17. This reveals a more rapid relaxation in tension than compression. Even when these curves are corrected for

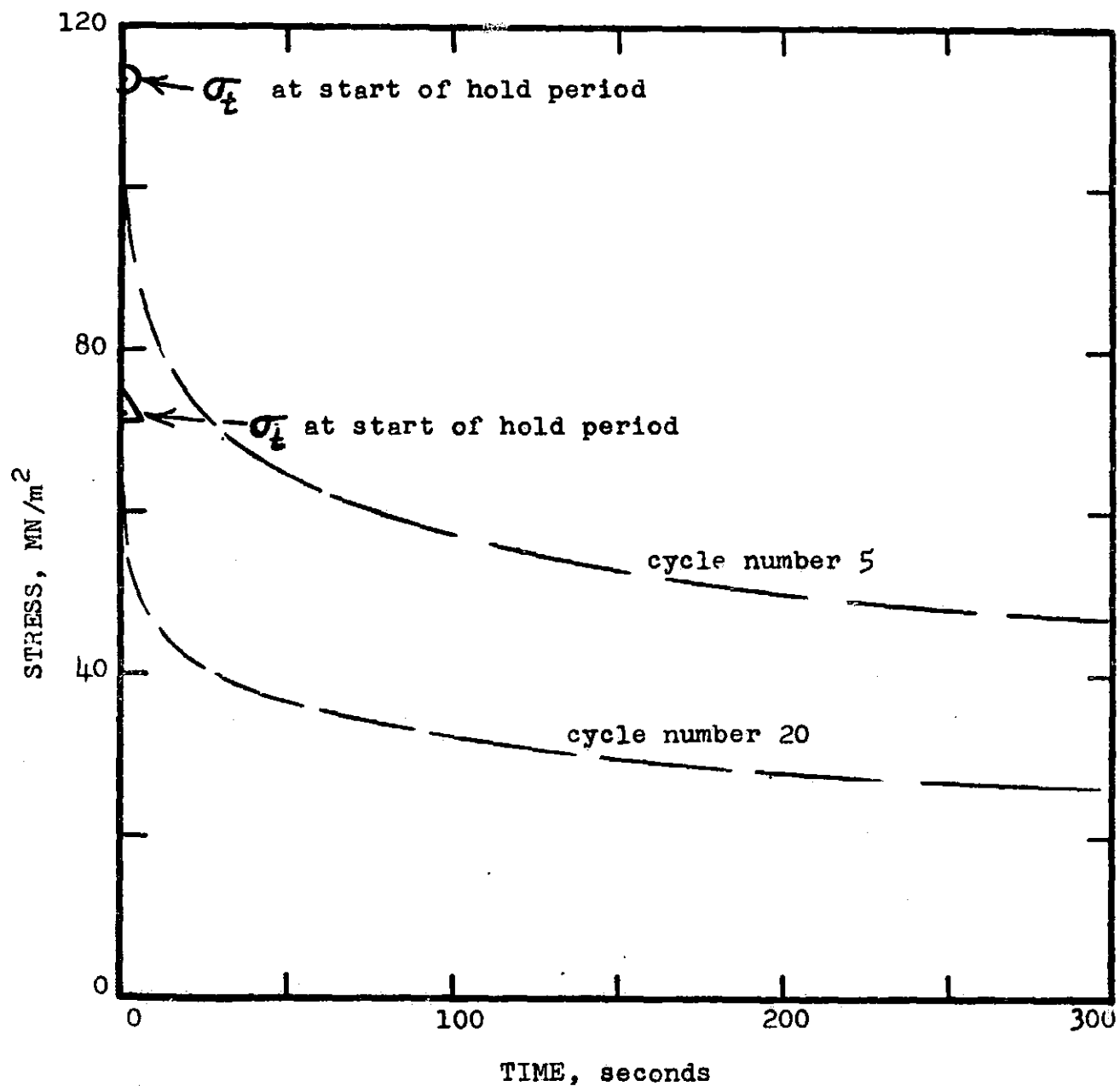


Figure 14- Relaxation curves plotted using data obtained from strip chart recording of load versus time behavior during hold-time test of Spec. No. R-2-67.

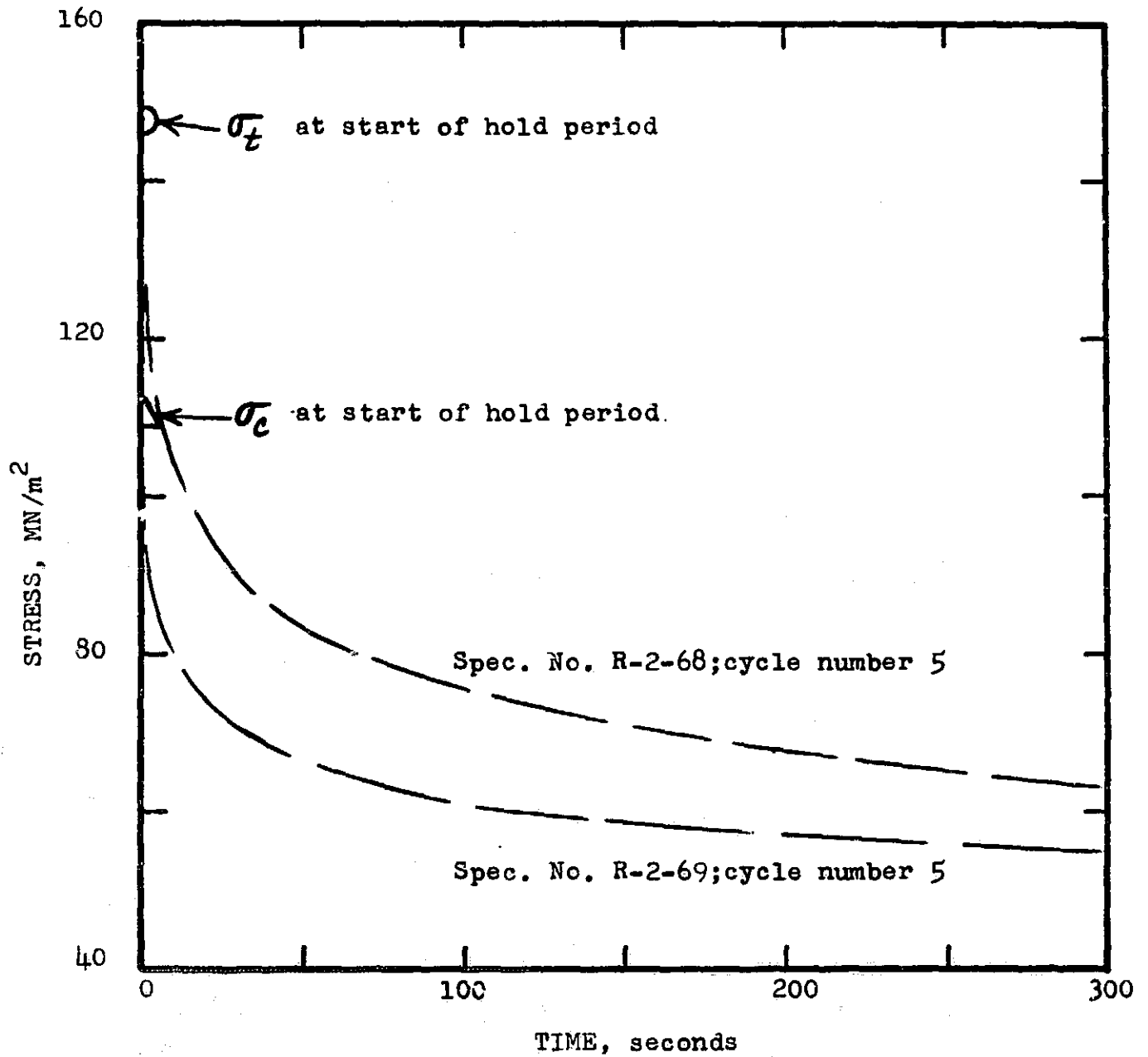


Figure 15- Relaxation curves plotted using data obtained from strip chart recording of load versus time behavior in hold-time tests.

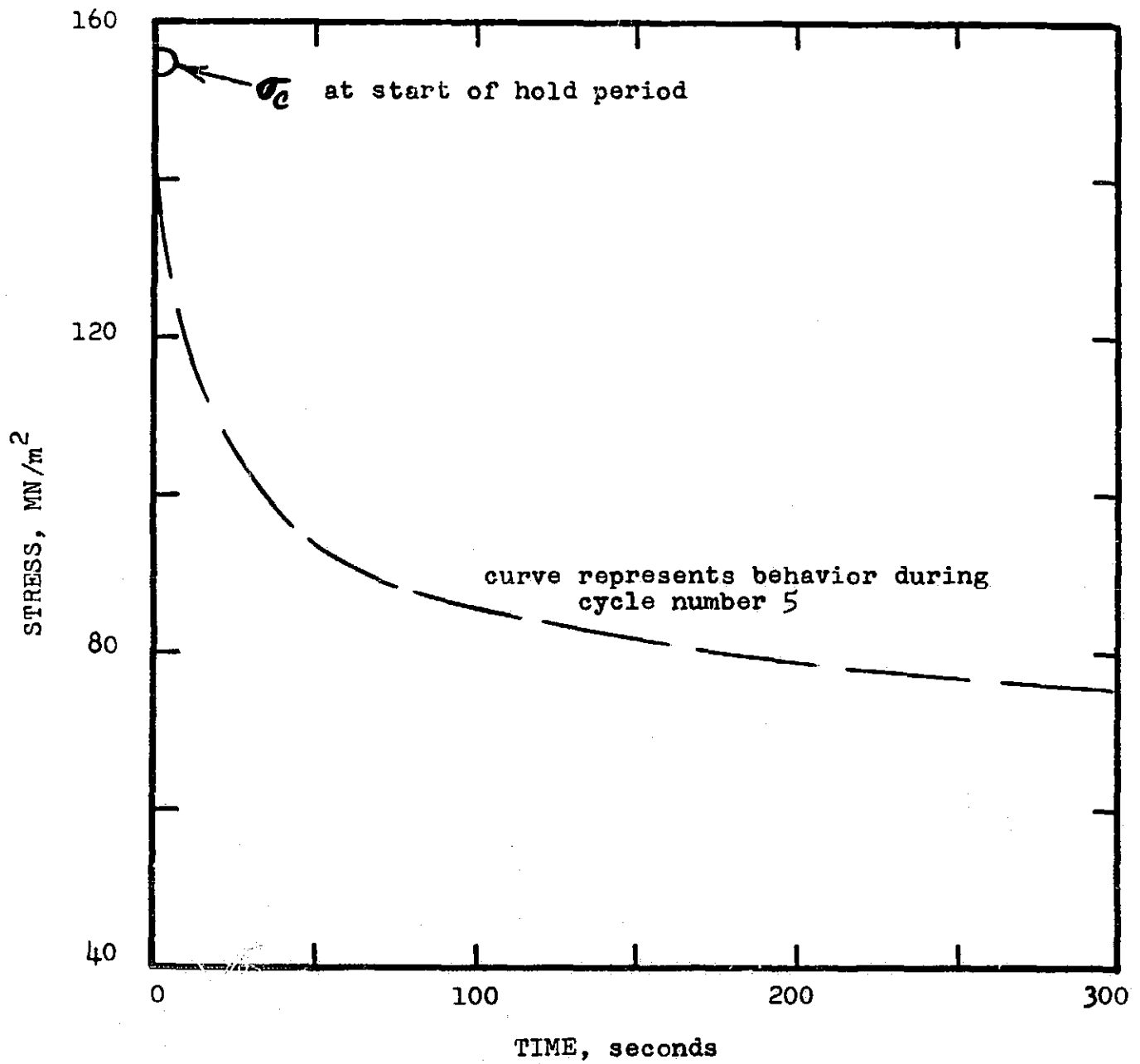


Figure 16- Relaxation curve plotted using data obtained from strip chart recording of load versus time behavior during hold-time test of Spec. No. R-2-72.

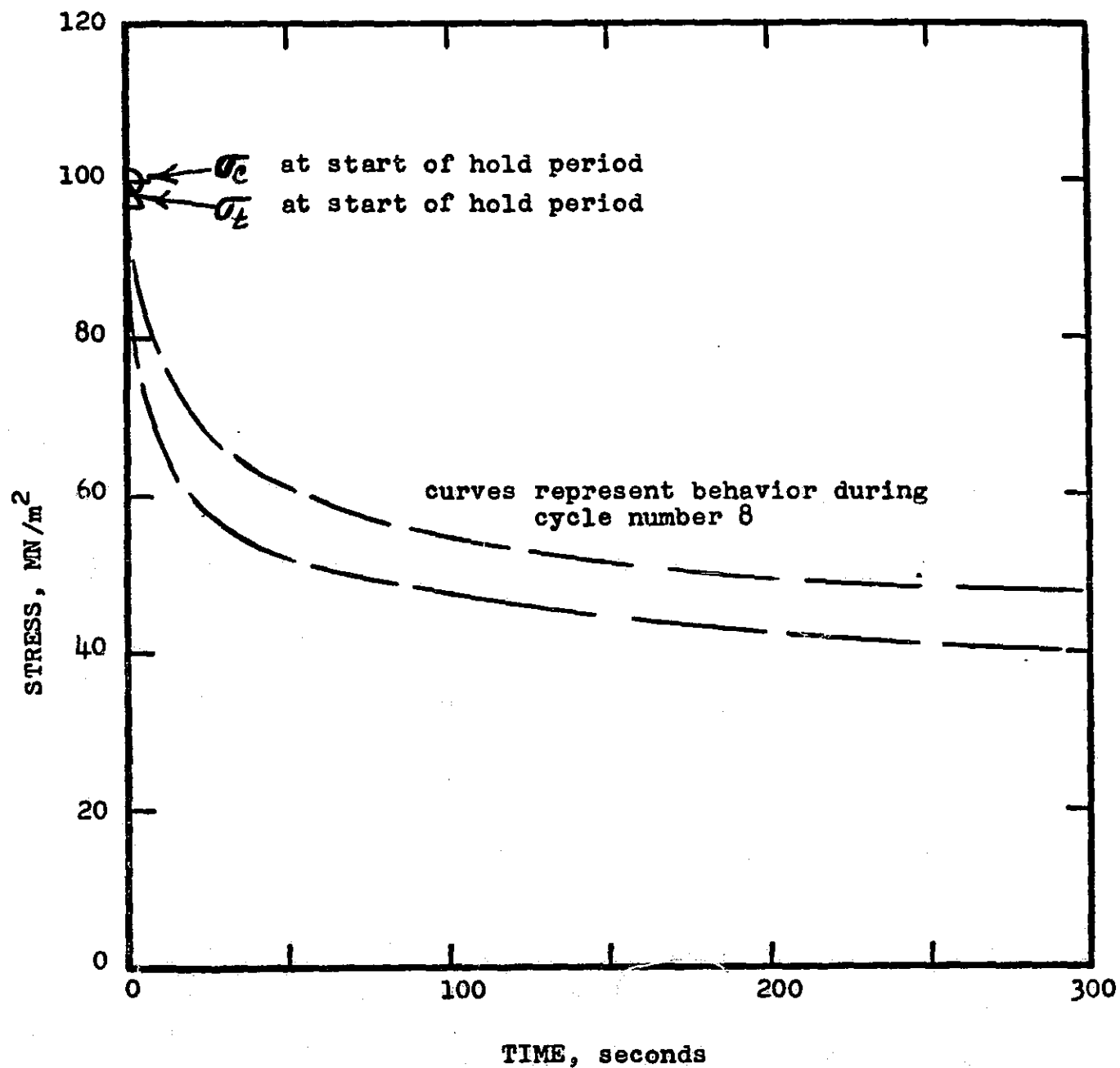


Figure 17- Relaxation curves plotted using data obtained from strip chart recording of load versus time behavior during hold-time test of Spec. No. R-2-73.

the different specimen diameters in tension and compression this conclusion still applies and the difference is quite appreciable. Comparing relaxation rates at a given stress level indicates that the rate in tension is about 1.5 times that in compression.

A preliminary analysis of some of the relaxation results plotted in Figures 14 through 17 was made in terms of a stress-rate ( $\dot{\sigma}$ ) divided by instantaneous stress type of correlation (see, "Analysis of the Relaxation Behavior of AISI 304 and 316 Stainless Steel at Elevated Temperature", by J. B. Conway, GE MP-730, 1969). The data for Cycle Nos. 5 and 20 from Figure 14 were employed and were found to yield very consistent results as shown in Figure 18. One point from R-2-68 is included and it too is found to be in close agreement with the R-2-67 data. This observation, while interesting, is based on only a limited analysis and should be viewed in this light. It does, however, suggest that a more detailed evaluation might be rewarding.

### C) Thermal-Mechanical Testing

Two special tests of the R-2 material were performed in argon to provide a limited assessment of the effect of combined temperature and mechanical strain cycling. Both tests involved a mechanical strain range of 3.5% and in both tests the temperature was cycled (linear rate of temperature change with a triangular wave form) between 538° and 260°C in each strain cycle. In the first test the phase relation between temperature and strain was chosen so that the maximum temperature (i.e. 538°C) occurred at the peak compression strain point in each cycle and the minimum temperature (i.e. 260°C) occurred at the peak tensile strain point in each cycle. In the second test the reversed phase relation was employed so that the maximum temperature occurred at the peak tensile strain point and the minimum temperature occurred at the peak compression strain point in each cycle. A summary of the test results obtained in these tests is presented in Table 7. A plot of the fatigue life obtained is shown in Figure 19 to compare these results with those for the R-2 alloy at 538°C reported in Task 2. It will be noted that the fatigue life values observed in these thermal-mechanical tests are lower than those indicated by the isothermal data at 538°C. Since the strain rate in the thermal-mechanical tests was  $8.75 \times 10^{-5} \text{ sec}^{-1}$  some of this reduction in fatigue life might be attributed to this factor. However, in Task 2 (see data points in Figure 19) the tests at a strain rate of  $4 \times 10^{-4} \text{ sec}^{-1}$  did not reveal a significant strain rate effect compared to the data at a strain rate of  $2 \times 10^{-3} \text{ sec}^{-1}$ . For this reason it seems reasonable to conclude that a certain thermal-mechanical effect seems to be in evidence. It also appears that the more detrimental condition corresponds to the maximum temperature occurring at the peak tension point in the strain cycle. Since some dimensional instability was observed in these tests these conclusions must be viewed with some reservation in light of the discussion presented in the section on hold-time effects.

Typical hysteresis loops for these tests are presented in

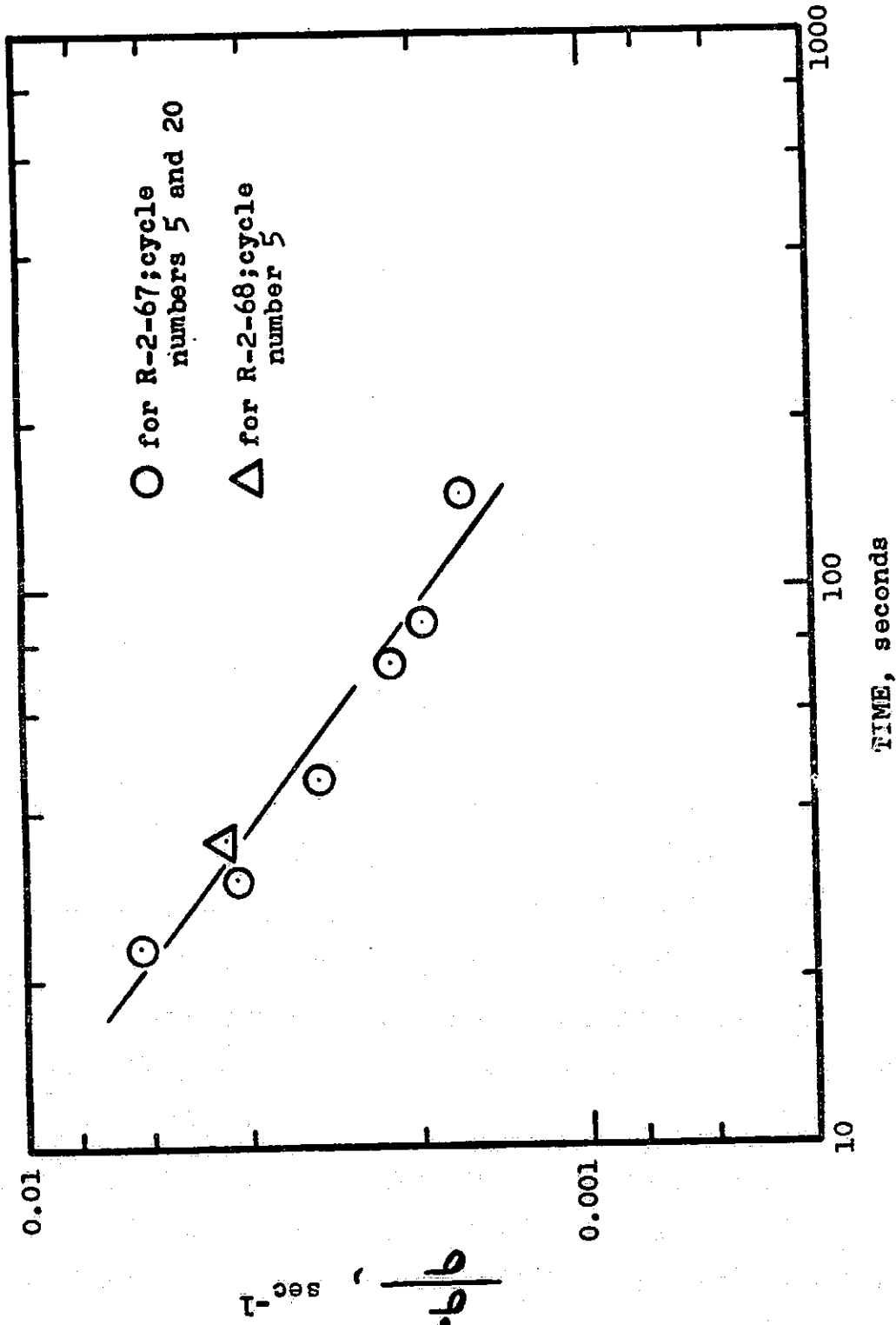


Figure 18- Stress rate correlation of relaxation data obtained in hold-time tests of Spec. Nos. R-2-67 and R-2-68.

**Table 7 - Combined Thermal-Mechanical Strain Cycling Test Results Obtained in Argon**  
 Using a Temperature Cycle from 538° to 260°C; Cyclic Frequency was 4.5 cph

R-2 Series Zirconium Copper (1/2 Hard)		Total Mechanical Strain Range = 3.5%	Axial Strain Control A - ratio of infinity E = 80.7 x 103 MN/m <sup>2</sup> at 538°C		# Nf, cycles to failure				
Spec. No.	Peak Temp. Location	First Cycle				Near Nf/2			
		Peak Stress, MN/m <sup>2</sup>	Stress at Peak Strain, MN/m <sup>3</sup>	Stress Range based on endpoints, MN/m <sup>2</sup>	Peak Stress, MN/m <sup>2</sup>	Stress at Peak Strain MN/m <sup>2</sup>	Stress Range based on endpoints, MN/m <sup>2</sup>		
R-2-61	Compression	238 C	163.5C	517	96.5 C	68.95 C	165.5	284	
R-2-62	Tension	217 T	151.7T	417	84T	58.6T	158.5	188	
Note: Poisson's ratio at 538°C was 0.35 in both tests * A slight barrelling was observed in R-2-61 and a slight necking was observed in R-2-62.									



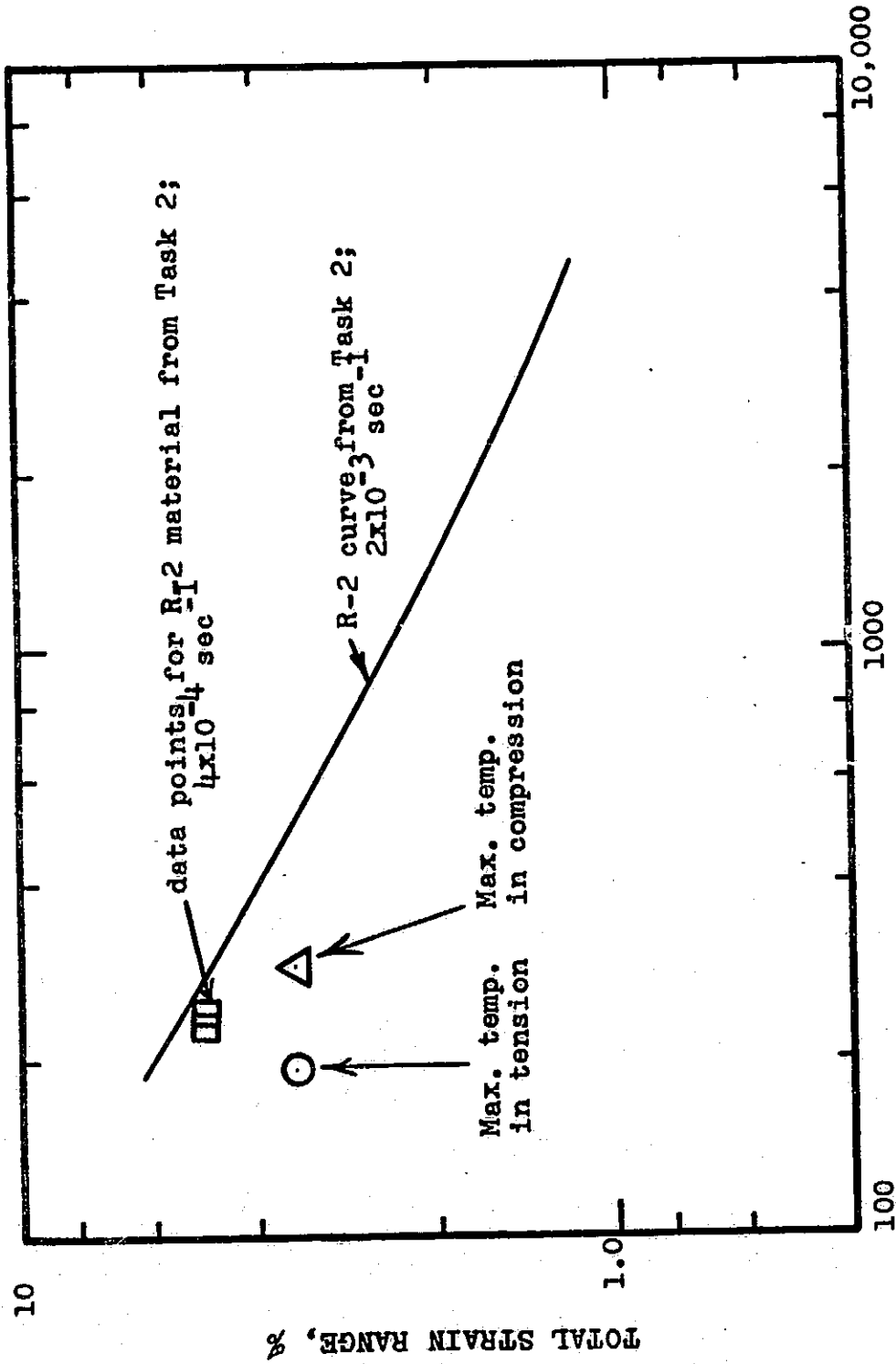


Figure 19- Thermal-mechanical test points compared to isothermal fatigue data for R-2 material at 538°C.

Figures 20 and 21. In Figure 20 the loops for the first few cycles reveal the characteristic behavior observed in this type of testing. A maximum in the load trace is always obtained much before the peak temperature point and this results from the effect of temperature on material strength. A similar behavior pattern was obtained in the test of Spec. No. R-2-61 except that the effect was observed in the compression portion of the cycle.

In Figures 20 and 21 the temperature scale provided allows the temperature at each position within the cycle to be identified. A vertical projection from this temperature scale to a point on the hysteresis loop enables the temperature at this location in the cycle to be determined.

A decided cyclic strain softening was observed in these tests as evidenced in the hysteresis loops shown in Figure 20. This is, of course, the same type of behavior noted in the isothermal tests of this alloy.

The trend in the data obtained in these thermal-mechanical strain cycling tests along with the general trend observed in the hold-time tests is consistent with the behavior pattern to be expected based on the concept of strainrange partitioning (see S. S. Manson, "The Challenge to Unify Treatment of High Temperature Fatigue -- A Partisan Proposal Based on Strainrange Partitioning", ASTM STP-520, 1973, p. 744-755).

## VII - CONCLUSIONS

This report has presented and discussed the test results obtained during the Task 3 portion of this contract and presents the final report for this program. Following the evaluation of twelve candidate materials on Task 1 of this program and the more detailed evaluation of one of these materials (zirconium-copper, 1/2 Hard, alloy) within the Task 2 effort, some further special tests of the Task 2 material were performed within the Task 3 portion of the program. In addition, the Task 3 effort focused on an evaluation of the short-term tensile and low-cycle fatigue properties of a second lot of the zirconium-copper, 1/2 Hard, material.

A series of tests was performed to evaluate the smooth bar and notched bar fatigue life of the zirconium-copper, 1/2 Hard, alloy tested in air at room temperature in axial strain control. These data indicated that the ratio of the smooth bar fatigue life to the notched bar fatigue life was constant at a value of about 6.0 over the cyclic life regime studied.

Some additional hold-time tests of the zirconium-copper, 1/2 Hard, material were performed in an evaluation of the effect of a 300-second hold period duration. Tests were performed using a hold period in tension only, compression only, and in both tension and compression. A decided dimensional instability was observed in these specimens which precluded a reliable assessment of hold-time effects.

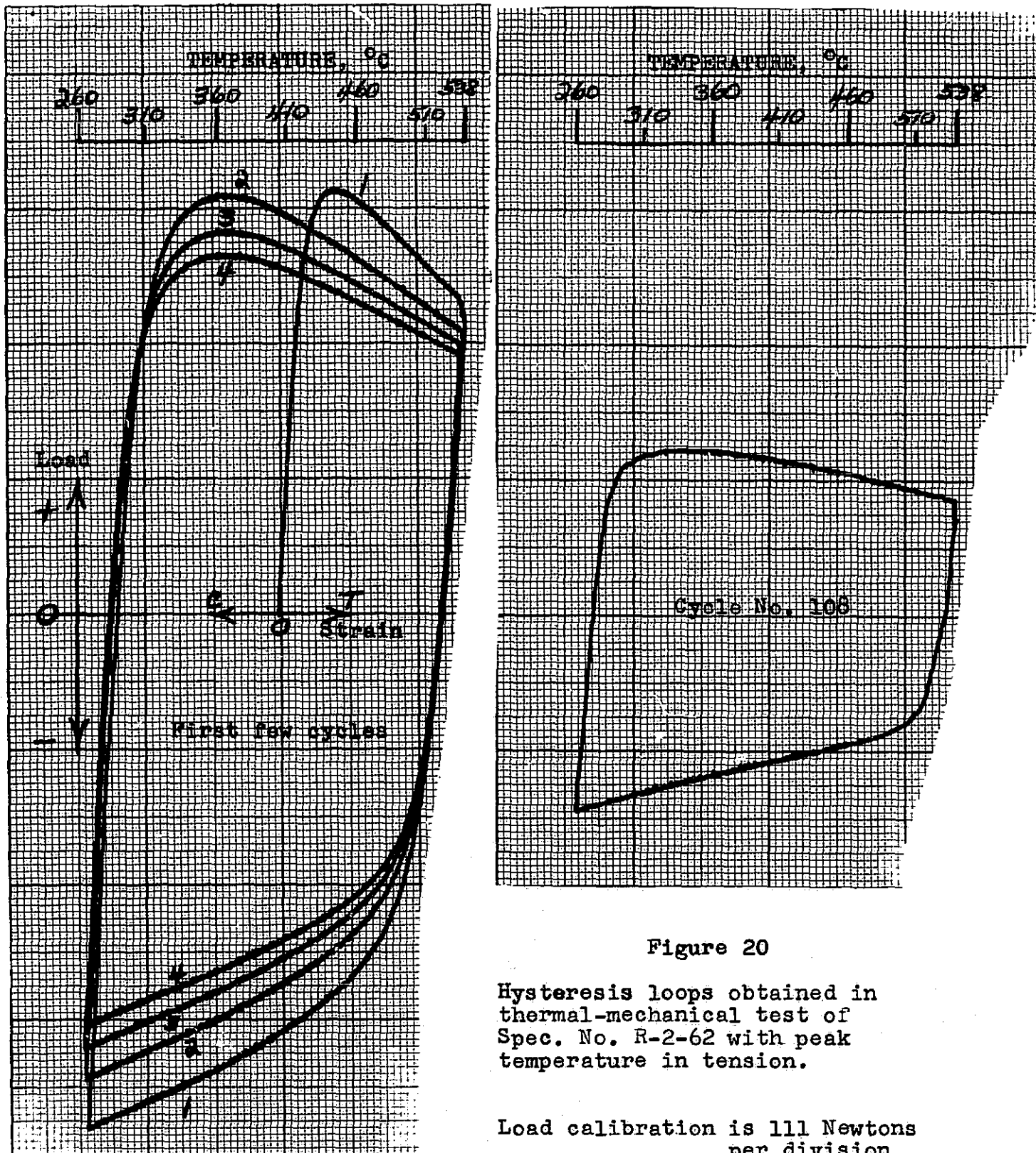


Figure 20

Hysteresis loops obtained in thermal-mechanical test of Spec. No. R-2-62 with peak temperature in tension.

Load calibration is 111 Newtons per division

Strain calibration is 0.0625 % per division

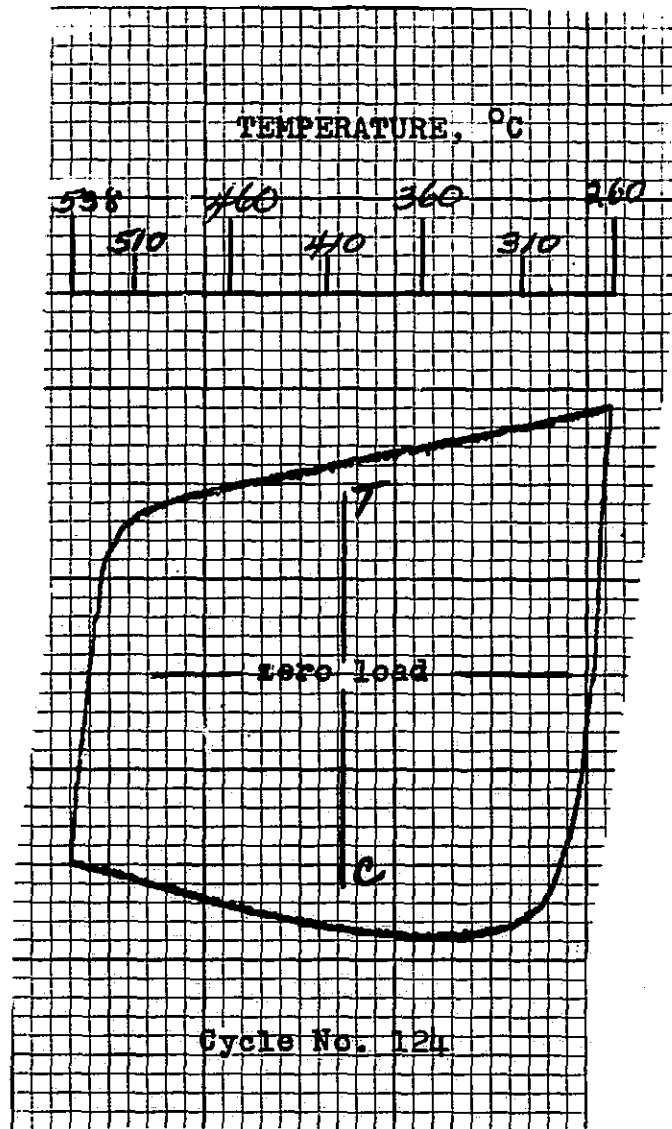


Figure 21- Hysteresis loop obtained in thermal-mechanical test of Spec. No. R-2-61 with peak temperature in compression.

Load calibration is 222 Newtons per division  
Strain calibration is 0.125% per division

Relaxation data obtained in the first few (up to 20) cycles of these hold-time tests were analyzed and some interesting observations were made. One of these pertained to the indication that the relaxation rate in tension is noticeably greater than that observed in compression. The other observation involved an indication that a fairly consistent correlation is obtained in terms of instantaneous stress rate divided by instantaneous stress.

Two thermal-mechanical strain cycling tests were performed in order to obtain a limited evaluation of this type of test on the fatigue life of the zirconium-copper alloy. A mechanical strain range of 3.5% was employed using a cyclic frequency of 4.5 cycles per hour and a cyclic temperature interval from 260° to 538°C. Both tests indicated a slight reduction in fatigue life compared to the isothermal data at 538°C. It was also indicated that the condition involving the maximum temperature occurring at the peak tensile strain point in the cycle was more detrimental than the reversed phase relation.

A second lot of the zirconium-copper, 1/2 Hard, material was evaluated and these results were compared to the data obtained for the first lot of this alloy. It was found that the second lot of this alloy exhibited noticeably lower yield and ultimate strengths at both room temperature and 538°C although the fatigue life at 538°C was essentially identical to that observed in the previously tested lot of this zirconium-copper alloy.